

Subspace-Based Localization of Far-Field and Near-Field Signals Without Eigendecomposition

Weiliang Zuo, Jingmin Xin , *Senior Member, IEEE*, Nanning Zheng, *Fellow, IEEE*, and Akira Sano, *Member, IEEE*

Abstract—We propose a new subspace-based localization of far-field (FF) and near-field (NF) narrowband signals (LOFNS) without eigendecomposition impinging on a symmetrical uniform linear array, where the oblique projection operator is utilized to isolate the NF signals from the FF ones, and the procedures of computationally burdensome eigendecomposition are not required in the estimation of the NF and FF location parameters and the computation of oblique projection operator. As a measure against the impact of finite array data, an alternating iterative scheme is presented to improve the estimation accuracy of the oblique projection operator and, hence, that of the NF location parameters, where the “saturation behavior” encountered in most of localization methods is overcome. Furthermore, the statistical analysis of the proposed LOFNS is studied, and the asymptotic mean-squared-error expressions of the estimation errors are derived for the FF and NF location parameters. Finally, the effectiveness and the theoretical analysis of the proposed LOFNS are substantiated through numerical examples, and the simulation results demonstrate that the LOFNS provides remarkable and satisfactory estimation performance for both the NF and FF signals compared with some existing localization methods even with eigendecomposition.

Index Terms—Direction-of-arrival, far-field, near-field, oblique projection, source localization, uniform linear array.

I. INTRODUCTION

LOCALIZATION of the multiple narrowband signals impinging on an array of sensors is a fundamental problem in many applications (see, e.g. [1]–[4] and references therein), where the plane-wave model characterized by only the direction-of-arrival (DOA) or the spherical-wave model parameterized by the DOA and the range are considered for the incident signals located in far-field (FF) or near-field (NF), respectively. In the array processing literature, numerous localization methods were studied for the FF signals (e.g., [5]–[11]) or the NF ones (e.g., [12]–[23]), where the pair-matching (i.e., association) of the estimated DOAs and ranges is usually required in the latter. However, in some practical scenarios (for example, speaker

localization with microphone arrays) (e.g., [24]–[26]), the FF signals and the NF ones usually coexist, and the aforementioned methods only based on the plane-wave or spherical-wave model deteriorate dramatically, and hence the localization of these mixed signals has received considerable attention.

Recently the localization of the mixed FF and NF signals were investigated from different aspects, and most of them (i.e., [30]–[43]) generally consist of three major stages: (i) the DOA estimation of FF signals, (ii) the isolation of the NF signals from the FF ones with the matrix differencing or oblique projection technique, and (iii) the DOA and range estimation of NF signals, where the crux is the separation (i.e., isolation). Some higher-order statistics (HOS) or cyclostationarity based localization methods [29]–[35] were presented by exploiting the specifically temporal properties of incident signals (e.g., [27], [28]), but they often require many array snapshots and have high computational load. Several differencing methods were suggested to eliminate the contribution of the FF signals and the additive noises in the NF localization [36]–[38], but the required structure property of the signal covariance matrix is only valid for large number of snapshots. By utilizing the geometric configuration of a symmetrical uniform linear array (ULA), some subspace-based methods with second-order statistics (SOS) were proposed for the mixed incident signals [39]–[43]. The generalized ESPRIT and polynomial rooting (GESPR) [39] performs worse, because the generalized ESPRIT (GESPRIT) [44] encounters ambiguity in some scenarios owing to the selection of weighting matrix (cf. [45]), and it results in spurious peaks for more than one FF signals. The method [40] requires two-dimensional MUSIC-like spectrum peak searching, and a subjective criterion is needed to distinguish the FF and NF signals. Further some other methods were presented [41]–[43], where the NF and FF signals are separated with oblique projection, which is an extended orthogonal projection and used in the DOA estimation of the mixed noncoherent and coherent FF signals (cf., [46]–[49], [67]–[71]). In the oblique projection based MUSIC (OPMUSIC) [41], the DOAs of FF signals are estimated by finding the peaks of the MUSIC-like one-dimensional (1D) spectrum obtained from the array covariance matrix, and then the oblique projection technique [47] is adopted to separate the NF signals from the FF signals by using the estimated DOAs of FF signals, while the DOAs of NF signals are estimated by finding the peaks of the MUSIC-like 1D spectrum obtained from the Hankel matrix constructed with the anti-diagonal elements of the projected array covariance matrix, and by using these estimated DOAs, the ranges of the corresponding NF signals are estimated by finding the peaks of another MUSIC-like 1D spectrum obtained from the array covariance matrix. Obviously the major computational complexity of the OPMUSIC is dominated by not only the computations of array covariance matrix and the projected

Manuscript received February 8, 2018; revised May 25, 2018; accepted June 19, 2018. Date of publication July 11, 2018; date of current version July 30, 2018. The associate editor coordinating the review of this manuscript and approving it for publication was Prof. Mark A. Davenport. This work was supported in part by the National Natural Science Foundation of China under Grants 61671373 and 61790563, and in part by the Programme of Introducing Talents of Discipline to Universities under Grant B13043. This paper was presented in part at the IEEE 39th International Conference on Acoustics, Speech, and Signal Processing, Florence, Italy, May 2014. (*Corresponding author: Jingmin Xin.*)

W. Zuo, J. Xin, and N. Zheng are with the National Engineering Laboratory of Visual Information Processing and Applications and the Institute of Artificial Intelligence and Robotics, School of Electronic and Information Engineering, Xi'an Jiaotong University, Xi'an 710049, China (e-mail: weiliangzuo@stu.xjtu.edu.cn; jxin@mail.xjtu.edu.cn; nnzheng@mail.xjtu.edu.cn).

A. Sano is with the Department of System Design Engineering, Keio University, Yokohama 223-8522, Japan (e-mail: sano@sd.keio.ac.jp).

Digital Object Identifier 10.1109/TSP.2018.2853124

array covariance matrix and their eigendecompositions but also by three peak picking procedures of the MUSIC-like spectra, where the precise peak searching necessitates fine grid interval but is rather time-consuming task with heavy computation load. The sparse recovery and oblique projection based method (SROP) [42] needs to solve the convex optimization problems and has a difficulty to determine the regularization parameter that balances the tradeoff between the Frobenius and ℓ_1 -norm terms. The oblique projector based MUSIC-GESPRIT (OPMUGE) [43] estimates the DOAs of FF and NF signals with two different procedures of MUSIC- and GESPRIT-like spectrum searching and estimates the range of NF signals by the polynomial rooting in the compressed searching area, yet it suffers from degradation as mentioned above [45]. Unfortunately, when the number of snapshots is not large sufficiently, the off-diagonal influence in the sample signal covariance matrix and the erroneous estimated oblique projector usually causes the “saturation behavior” in the localization of NF signals regardless of the signal-to-noise ratio (SNR), where the estimated DOAs and ranges have high elevated error floors, which do not decrease with the increasing SNR. Although we proposed a localization method for the mixed signals [50], it was applicable only for one NF signal. Moreover, most of the aforementioned localization methods require the eigendecomposition procedure, which is computationally intensive and time-consuming, when the number of sensors is large (cf. [51], [10], [11]).

Therefore, in this paper, we propose a new oblique projection and subspace based localization of the FF and NF signals (LOFNS) impinging on a ULA with symmetrical geometric configuration in a computationally efficient way, where the eigendecomposition and pair-matching processes are avoided. Firstly the DOAs of FF signals are estimated from the array correlation matrix through a linear operator, and then the oblique projection operator is calculated with these estimates to isolate the NF signals from the FF ones. Thirdly the DOAs of NF signals are estimated from a Toeplitz correlation matrix through another linear operator, and hereafter the ranges of NF signals are obtained from the array covariance matrix through a polynomial rooting with the corresponding estimated DOA. Further as a measure against the impact of finite array data, an alternating iterative scheme is presented to improve the estimation accuracy of the oblique projection operator and that of the NF location parameters, where the aforementioned “saturation behavior” is alleviated. The statistical properties of the LOFNS are analyzed, and asymptotic mean-squared-error (MSE) expressions of the estimation errors are derived for the FF and NF signals. Evidently compared with the OPMUSIC [41], the proposed LOFNS has the following main differences: (i) the eigendecomposition procedure is avoided by using the linear operation in DOA and range estimation, (ii) the eigendecomposition procedure is also avoided by using QR decomposition in the computation of oblique projection operator in a different way, (iii) an iterative method is proposed to alleviate the “saturation behavior”, and (iv) the asymptotic MSE expressions of the estimation errors are clarified explicitly. Finally, the effectiveness and the theoretical analysis of the LOFNS are substantiated through numerical examples, and the simulation results demonstrate that the LOFNS performs well for both the FF and NF signals at relatively low SNR and with a small number of snapshots.

Notation: Throughout the paper, $\mathbf{O}_{m \times n}$, \mathbf{I}_m , \mathbf{J}_m , $\mathbf{0}_{m \times 1}$, and $\delta_{n,t}$ stand for an $m \times n$ null matrix, $m \times m$ identity matrix, $m \times m$ counter-identity matrix, $m \times 1$ null vector, and Kronecker delta, while $E\{\cdot\}$, $\{\cdot\}^*$, $(\cdot)^T$, and $(\cdot)^H$ represent the

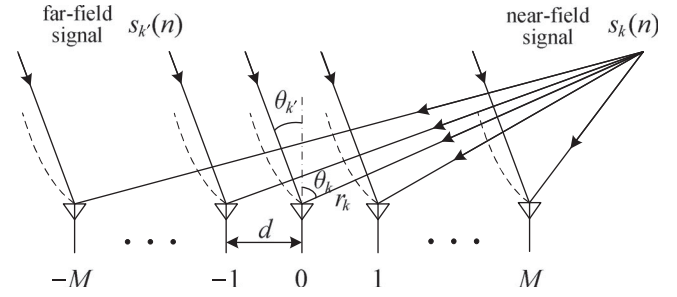


Fig. 1. The geometric configuration of the symmetrical ULA and the propagations of the FF and NF signals.

statistical expectation, complex conjugate, transposition, and Hermitian transposition, respectively. Additionally, $\rho(\cdot)$, $(\cdot)^\dagger$, $\det\{\cdot\}$, $\mathcal{R}(\cdot)$, and $\mathcal{N}(\cdot)$ indicate the rank, Moore-Penrose pseudoinverse, determinant, the range space, and null space of the bracketed matrix, while $\text{diag}(\cdot)$ and $\text{blkdiag}(\cdot)$ denote the diagonal matrix or block diagonal matrix operator. Further \otimes , $\text{tr}\{\cdot\}$, \oplus , and \cap signify the Kronecker product, the trace operator, the direct sum operator, and the intersection operator, while $\text{Re}\{\cdot\}$ denotes the real part of the bracketed quantity, $\text{vec}(\mathbf{X})$ is a matrix operation stacking the columns of a matrix \mathbf{X} one under the other to form a single column, and $\mathcal{O}[\cdot]$ indicates the order of magnitude.

II. PROBLEM STATEMENT

A. Data Model and Basic Assumptions

As shown Fig. 1, there are K noncoherent mixed FF and NF narrowband signals $\{s_k(n)\}$ impinging on the ULA, which consists of $2M + 1$ omnidirectional sensors with spacing d and indexed by $m = -M, \dots, -1, 0, 1, \dots, M$, where the K_1 signals $\{s_k(n)\}_{k=1}^{K_1}$ are in the FF with the location parameters $\{(\theta_k, \infty)\}_{k=1}^{K_1}$, and the other K_2 signals $\{s_k(n)\}_{k=K_1+1}^K$ are in the NF with the location parameters $\{(\theta_k, r_k)\}_{k=K_1+1}^K$, while θ_k is the DOA of $s_k(n)$ measured at the reference sensor relative to the normal of array, r_k is the corresponding range between the signal source and the reference sensor, where $K = K_1 + K_2$. By letting the center of ULA (i.e., sensor 0) be the phase reference point, the noisy data $x_m(n)$ received at the m th sensor is given by

$$x_m(n) = \sum_{k=1}^K s_k(n) e^{j\tau_{mk}} + w_m(n) \quad (1)$$

where $w_m(n)$ is the additive noise, and τ_{mk} indicates the phase delay of the k th signal $s_k(n)$ due to the propagation time between the reference sensor and the m th sensor. For the NF signal located in the Fresnel region $r_k \in (0.62(D^3/\lambda)^{1/2}, 2D^2/\lambda)$ [4], [52], τ_{mk} can be approximated by the second-order Taylor expansion as [12], [13], [15], [19]

$$\tau_{mk} \approx m\psi_k + m^2\phi_k \quad (2)$$

where ψ_k and ϕ_k are called as the electric angles given by

$$\psi_k \triangleq -\frac{2\pi d}{\lambda} \sin \theta_k \quad (3)$$

$$\phi_k \triangleq \frac{\pi d^2}{\lambda r_k} \cos^2 \theta_k \quad (4)$$

in which λ is the wavelength of incident signals, while D is the aperture of array given by $D = 2Md$ herein. Otherwise, for the FF signal lies in the Fraunhofer region $r_k \in (2D^2/\lambda, \infty)$ [4], [52], τ_{mk} is parameterized by only the DOA θ_k and approximated as [12], [14]

$$\tau_{mk} \approx m\psi_k. \quad (5)$$

Then the received array data in (1) can be rewritten compactly

$$\mathbf{x}(n) = \mathbf{A}\mathbf{s}(n) + \mathbf{w}(n) \quad (6)$$

where $\mathbf{x}(n)$, $\mathbf{s}(n)$, and $\mathbf{w}(n)$ are the vectors of the received data, the incident signals and the additive noises given by $\mathbf{x}(n) \triangleq [x_{-M}(n), \dots, x_{-1}(n), x_0(n), x_1(n), \dots, x_M(n)]^T$, $\mathbf{s}(n) \triangleq [\mathbf{s}_f^T(n), \mathbf{s}_n^T(n)]^T$, $\mathbf{s}_f(n) \triangleq [s_1(n), s_2(n), \dots, s_{K_1}(n)]^T$, $\mathbf{s}_n(n) \triangleq [s_{K_1+1}(n), s_{K_1+2}(n), \dots, s_K(n)]^T$, and $\mathbf{w}(n) \triangleq [w_{-M}(n), \dots, w_{-1}(n), w_0(n), w_1(n), \dots, w_M(n)]^T$, while \mathbf{A} is the array response matrix given by $\mathbf{A} \triangleq [\mathbf{A}_f, \mathbf{A}_n]$, where $\mathbf{A}_f \triangleq [\mathbf{a}_f(\theta_1), \mathbf{a}_f(\theta_2), \dots, \mathbf{a}_f(\theta_{K_1})]$, $\mathbf{A}_n \triangleq [\mathbf{a}_n(\theta_{K_1+1}, r_{K_1+1}), \mathbf{a}_n(\theta_{K_1+2}, r_{K_1+2}), \dots, \mathbf{a}_n(\theta_K, r_K)]$, in which $\mathbf{a}_f(\theta_k) \triangleq [e^{-jM\psi_k}, \dots, e^{-j\psi_k}, 1, e^{j\psi_k}, \dots, e^{jM\psi_k}]^T$, and $\mathbf{a}_n(\theta_k, r_k) \triangleq [e^{-jM\psi_k} e^{jM^2\phi_k}, \dots, e^{-j\psi_k} e^{j\phi_k}, 1, e^{j\psi_k} e^{j\phi_k}, \dots, e^{jM\psi_k} e^{jM^2\phi_k}]^T$.

Here we make the basic assumptions as follows.

- A1) The array is calibrated, and the array response matrix \mathbf{A} has full rank and unambiguous.
- A2) The incident signals $\{s_k(n)\}$ are temporally complex white Gaussian random processes with zero-mean and the variance given by $E\{s_k(n)s_k^*(n)\} = r_{s_k} \delta_{n,t}$ and $E\{s_k(n)s_k(n)\} = 0, \forall n, t$.
- A3) The additive noises $\{w_m(n)\}$ are temporally and spatially complex white Gaussian random processes with zero-mean and the covariance matrices $E\{\mathbf{w}(n)\mathbf{w}^H(n)\} = \sigma^2 \mathbf{I}_{2M+1} \delta_{n,t}$, and $E\{\mathbf{w}(n)\mathbf{w}^T(n)\} = \mathbf{O}_{(2M+1) \times (2M+1)}, \forall n, t$. Additionally, the additive noises are independent to the incident signals.
- A4) The numbers of the FF and NF signals K_1 and K_2 are known (cf. [53]), and the number of all incident signals K satisfies the relation $K < M + 1$.
- A5) The sensor spacing d satisfies the relation $d \leq \lambda/4$ for avoiding the estimation ambiguity.

Remark A: In fact, the estimation of the number of FF signals and that of NF signals are necessitated, however this problem has not been studied in the literature of array processing to the best of our knowledge. We proposed an oblique projection based enumerator for the mixed noncoherent and coherent FF signals (OPEMS) in [53], where the computationally intensive and time-consuming eigendecomposition is avoided, and we would modify this number detection method [53] to the case of mixed FF and NF signals considered herein. Such an elaborate algorithm is currently under investigated. ■

B. Problem of Localizing Mixed Incident Signals

Under the basic assumptions, from (6), the array covariance matrix \mathbf{R} is given by

$$\mathbf{R} \triangleq E\{\mathbf{x}(n)\mathbf{x}^H(n)\} = \mathbf{A}\mathbf{R}_s\mathbf{A}^H + \sigma^2 \mathbf{I}_{2M+1} \quad (7)$$

where \mathbf{R}_s , \mathbf{R}_{s_f} , and \mathbf{R}_{s_n} are the covariance matrices of all incident signals, the FF signals, and the NF signals defined by

$$\mathbf{R}_s \triangleq E\{\mathbf{s}(n)\mathbf{s}^H(n)\} = \text{blkdiag}(\mathbf{R}_{s_f}, \mathbf{R}_{s_n}) \quad (8)$$

$$\mathbf{R}_{s_f} \triangleq E\{\mathbf{s}_f(n)\mathbf{s}_f^H(n)\} = \text{diag}(r_{s_1}, r_{s_2}, \dots, r_{s_{K_1}}) \quad (9)$$

$$\mathbf{R}_{s_n} \triangleq E\{\mathbf{s}_n(n)\mathbf{s}_n^H(n)\} = \text{diag}(r_{s_{K_1+1}}, \dots, r_{s_K}). \quad (10)$$

Obviously the range spaces $\mathcal{R}(\mathbf{A}_f)$ and $\mathcal{R}(\mathbf{A}_n)$ associated with the FF and NF signals are nonoverlapping (or disjoint) and not orthogonal, i.e., $\mathcal{R}(\mathbf{A}) = \mathcal{R}(\mathbf{A}_f) \oplus \mathcal{R}(\mathbf{A}_n)$ and $\mathcal{R}(\mathbf{A}_f) \cap \mathcal{R}(\mathbf{A}_n) = \{\mathbf{0}\}$, where the orthogonal projector cannot completely cancel the influence of the known DOAs on the estimation of the unknown ones [47]. Hence the localization of these mixed signals cannot be accomplished directly from \mathbf{R} in (7).

Thus in this paper, we investigate the problem of estimating the location parameters $\{\theta_k\}_{k=1}^K$ and $\{r_k\}_{k=K_1+1}^K$ of the FF and NF signals from finite array snapshots $\{\mathbf{x}(n)\}_{n=1}^N$ in a computationally efficient way, where the oblique projection operator is utilized to suppress the FF signals and to preserve the NF signals in the localization of the NF signals.

Remark B: The random matrix theory (RMT) [54], [55] is used to study the asymptotic behavior of the eigenvalues and eigenvectors of different random matrix models including the sample covariance matrix for solving the ‘‘threshold effect’’ of subspace-based direction estimation in the asymptotic situation, where both the numbers of snapshots and sensors are large and of the same order of magnitude (see, e.g., [56]–[59]). Herein we consider the subspace-based localization of the mixed FF and NF signals without eigendecomposition, where the number of sensors is not comparable in the same order of magnitude to that of snapshots. ■

III. SUBSPACE-BASED LOCALIZATION OF MIXED SIGNALS WITHOUT EIGENDECOMPOSITION

As depicted in Fig. 2, the proposed LOFNS consists of three major parts: (1) DOA estimation of the FF signals through a linear operator, (2) computation of oblique projection operator with accessible data, and (3) DOA and range estimation of NF signals with an alternating iterative scheme.

A. DOA Estimation of FF Signals

By partitioning the array covariance matrix \mathbf{R} in (7) as

$$\mathbf{R} = \begin{bmatrix} \mathbf{R}_{11} & \mathbf{R}_{12} \\ \mathbf{R}_{21} & \mathbf{R}_{22} \end{bmatrix} \begin{matrix} K \\ 2M+1-K \end{matrix} \quad (11)$$

the noise variance σ^2 is given by [60]

$$\sigma^2 = \frac{\text{tr}\{\mathbf{R}_{22}\mathbf{\Pi}\}}{\text{tr}\{\mathbf{\Pi}\}} \quad (12)$$

where $\mathbf{\Pi} = \mathbf{I}_{2M+1-K} - \mathbf{R}_{21}\mathbf{R}_{21}^\dagger$, and $\mathbf{R}_{21}^\dagger = (\mathbf{R}_{21}^H\mathbf{R}_{21})^{-1} \cdot \mathbf{R}_{21}^H$, we easily have the noiseless array covariance matrix $\bar{\mathbf{R}}$

$$\bar{\mathbf{R}} \triangleq \mathbf{R} - \sigma^2 \mathbf{I}_{2M+1} = \mathbf{A}\mathbf{R}_s\mathbf{A}^H. \quad (13)$$

By dividing the matrices \mathbf{A} and $\bar{\mathbf{R}}$ in (13) as $\mathbf{A} = [\mathbf{A}_1^T, \mathbf{A}_2^T]^T$ and $\bar{\mathbf{R}} = [\bar{\mathbf{R}}_1^T, \bar{\mathbf{R}}_2^T]^T$, where \mathbf{A}_1 (or $\bar{\mathbf{R}}_1$) and \mathbf{A}_2 (or $\bar{\mathbf{R}}_2$)

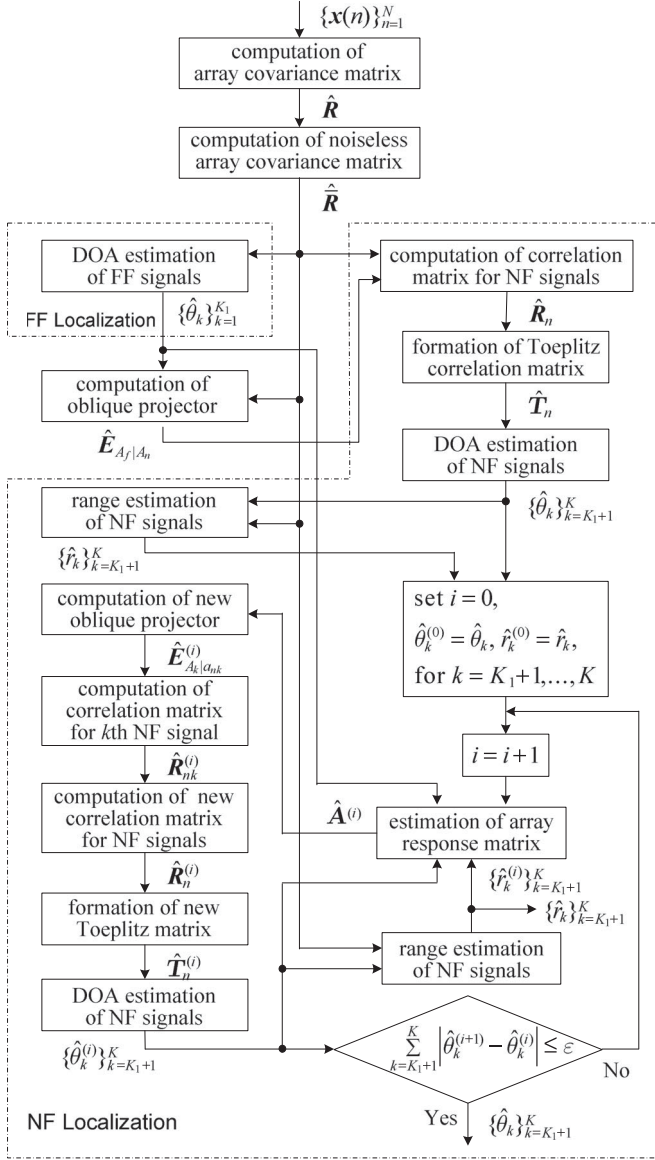


Fig. 2. The implementation flowchart of the proposed LOFNS.

consist of the first K and the last $2M + 1 - K$ rows of \mathbf{A} (or $\hat{\mathbf{R}}$), respectively, we can obtain a $K \times (2M + 1 - K)$ linear operator \mathbf{P} , which satisfies the following relation for DOA estimation (cf. [10], [11])

$$\mathbf{Q}^H \mathbf{A} = \mathbf{O}_{(2M+1-K) \times K} \quad (14)$$

i.e.,

$$\mathbf{Q}^H \mathbf{A}_f = \mathbf{O}_{(2M+1-K) \times K_1}, \quad \mathbf{Q}^H \mathbf{A}_n = \mathbf{O}_{(2M+1-K) \times K_2} \quad (15)$$

where $\mathbf{Q} \triangleq [\mathbf{P}^T, -\mathbf{I}_{2M+1-K}]^T$, and $\mathbf{P} = \mathbf{A}_1^{-H} \mathbf{A}_2^H = (\bar{\mathbf{R}}_1 \cdot \bar{\mathbf{R}}_1^H)^{-1} \bar{\mathbf{R}}_1 \bar{\mathbf{R}}_2^H$.

Thus when only finite array data are available, the sample array covariance matrix $\hat{\mathbf{R}}$ is given by

$$\hat{\mathbf{R}} = \frac{1}{N} \sum_{n=1}^N \mathbf{x}(n) \mathbf{x}^H(n) \quad (16)$$

where N is the number of snapshots, and the DOAs $\{\theta_k\}_{k=1}^{K_1}$ of the FF signals $\{s_k(n)\}_{k=1}^{K_1}$ can be estimated from $\hat{\mathbf{R}}$ by minimizing the following cost function

$$f(\theta) = \mathbf{a}_f^H(\theta) \mathbf{\Pi}_{\hat{\mathbf{Q}}} \mathbf{a}_f(\theta) \quad (17)$$

where

$$\mathbf{\Pi}_{\hat{\mathbf{Q}}} = \hat{\mathbf{Q}}(\hat{\mathbf{Q}}^H \hat{\mathbf{Q}})^{-1} \hat{\mathbf{Q}}^H \\ = \hat{\mathbf{Q}}(\mathbf{I}_{2M+1-K} - \hat{\mathbf{P}}^H (\hat{\mathbf{P}} \hat{\mathbf{P}}^H + \mathbf{I}_K)^{-1} \hat{\mathbf{P}}) \hat{\mathbf{Q}}^H \quad (18)$$

$$\hat{\mathbf{P}} = (\hat{\mathbf{R}}_1 \hat{\mathbf{R}}_1^H)^{-1} \hat{\mathbf{R}}_1 \hat{\mathbf{R}}_2^H \quad (19)$$

and $\hat{\mathbf{Q}} = [\hat{\mathbf{P}}^T, -\mathbf{I}_{2M+1-K}]^T$, in which $\mathbf{\Pi}_{\hat{\mathbf{Q}}}$ is calculated using the matrix inversion lemma implicitly, and the orthonormalization of the matrix $\hat{\mathbf{Q}}$ is used in $\mathbf{\Pi}_{\hat{\mathbf{Q}}}$ to improve the estimation performance [11].

Remark C: Theoretically the matrix \mathbf{A}_1 may have rank deficiency (i.e., $\rho(\mathbf{A}_1) < K$ or $\det\{\mathbf{A}_1\} = 0$) under very strictly circumstance, e.g., for a given NF signal, which locates at the position determined by the roots of the polynomial $\det\{\mathbf{A}_1\} = 0$ and only have $(K - 1)^2$ roots. However in practice, we can find that \mathbf{A}_1 is almost of full rank for a continuous space, especially for a small K . Further, we usually have the electric angle $\phi_k \ll 1$ [19] and hence \mathbf{A}_1 is nearly a Vandermonde matrix, which is of full rank under Assumption A1. ■

B. QR Decomposition Based Oblique Projection Operator

As described in Section II-B, the range spaces $\mathcal{R}(\mathbf{A}_f)$ and $\mathcal{R}(\mathbf{A}_n)$ of the FF and NF signals are nonoverlapping and not orthogonal, and hence the orthogonal projector cannot completely cancel the influence of the FF signals on the DOA estimation of the NF ones. Here we consider the utilization of the oblique projection technique (cf., [46]–[48]) to isolate the NF signals from the FF ones in a feasible manner.

The oblique projection operator $\mathbf{E}_{\mathbf{A}_f|\mathbf{A}_n}$ which projects onto the space $\mathcal{R}(\mathbf{A}_f)$ along a direction parallel to the space $\mathcal{R}(\mathbf{A}_n)$ is given by (e.g., [48])

$$\mathbf{E}_{\mathbf{A}_f|\mathbf{A}_n} \triangleq \mathbf{A}_f (\mathbf{A}_f^H \mathbf{\Pi}_{\mathbf{A}_n}^\perp \mathbf{A}_f)^{-1} \mathbf{A}_f^H \mathbf{\Pi}_{\mathbf{A}_n}^\perp \quad (20)$$

where

$$\mathbf{E}_{\mathbf{A}_f|\mathbf{A}_n} \mathbf{A}_f = \mathbf{A}_f, \quad \mathbf{E}_{\mathbf{A}_f|\mathbf{A}_n} \mathbf{A}_n = \mathbf{O}_{(2M+1) \times K_2} \quad (21)$$

and $\mathbf{\Pi}_{\mathbf{A}_n}^\perp$ is the orthogonal projector onto $\mathcal{N}(\mathbf{A}_n^H)$ defined by $\mathbf{\Pi}_{\mathbf{A}_n}^\perp \triangleq \mathbf{I}_{2M+1} - \mathbf{\Pi}_{\mathbf{A}_n}$, while $\mathbf{\Pi}_{\mathbf{A}_n} \triangleq \mathbf{A}_n (\mathbf{A}_n^H \mathbf{A}_n)^{-1} \mathbf{A}_n^H$. Unfortunately, the matrix \mathbf{A}_n in (20) for the NF signals $\{s_k(n)\}_{k=K_1+1}^K$ (i.e., $\mathbf{\Pi}_{\mathbf{A}_n}$ or $\mathbf{\Pi}_{\mathbf{A}_n}^\perp$) is unknown. Although there are several ways to calculate the oblique projector (e.g., [46]–[48]), herein we consider the computation of oblique projector with the QR decomposition (cf. [49], [53]), which factors a matrix into the product of a unitary matrix and an upper-triangular matrix and requires much lesser computational effort than the complete eigendecomposition (e.g., [51]).

By defining the orthogonal projector $\mathbf{\Pi}_{\mathbf{A}_f}^\perp$ onto $\mathcal{N}(\mathbf{A}_f^H)$ as $\mathbf{\Pi}_{\mathbf{A}_f}^\perp \triangleq \mathbf{I}_{2M+1} - \mathbf{A}_f (\mathbf{A}_f^H \mathbf{A}_f)^{-1} \mathbf{A}_f^H$, from (13), we easily get a new matrix $\tilde{\mathbf{R}}$ as

$$\tilde{\mathbf{R}} \triangleq \bar{\mathbf{R}} \mathbf{\Pi}_{\mathbf{A}_f}^\perp = \mathbf{A}_n \mathbf{R}_{sn} \mathbf{A}_n^H \mathbf{\Pi}_{\mathbf{A}_f}^\perp \quad (22)$$

where $\tilde{\mathbf{R}}$ only contains the information of the NF signals with $\rho(\tilde{\mathbf{R}}) = K_2$, and its QR decomposition is given by [51], [49]

$$\tilde{\mathbf{R}}\tilde{\mathbf{\Pi}} = \check{\mathbf{Q}}\check{\mathbf{R}} = \check{\mathbf{Q}}_1\check{\mathbf{R}}_1 \quad (23)$$

in which the unitary matrix $\check{\mathbf{Q}}$ is defined by $\check{\mathbf{Q}} \triangleq [\check{\mathbf{Q}}_1, \check{\mathbf{Q}}_2]$ with $\check{\mathbf{Q}}_1 \triangleq [\check{\mathbf{q}}_1, \check{\mathbf{q}}_2, \dots, \check{\mathbf{q}}_{K_2}]$ and $\check{\mathbf{Q}}_2 \triangleq [\check{\mathbf{q}}_{K_2+1}, \check{\mathbf{q}}_{K_2+2}, \dots, \check{\mathbf{q}}_{2M+1}]$, and the upper-triangular matrix $\check{\mathbf{R}}$ is given by $\check{\mathbf{R}} = [\check{\mathbf{R}}_1^T, \mathbf{O}_{(2M+1-K_2) \times (2M+1)}^T]^T$ with the $K_2 \times (2M+1)$ upper-triangular and full row rank matrix $\check{\mathbf{R}}_1$, while $\tilde{\mathbf{\Pi}}$ is the $(2M+1) \times (2M+1)$ permutation matrix, which does not change the correlation of the columns in $\check{\mathbf{Q}}$ (cf. [51]). Then from (23), $\mathbf{\Pi}_{\mathcal{A}_n}^\perp$ in (20) can be obtained as (cf. [Appendix A, 49])

$$\mathbf{\Pi}_{\mathcal{A}_n}^\perp = \mathbf{\Pi}_{\check{\mathbf{Q}}_1}^\perp = \check{\mathbf{Q}}_2\check{\mathbf{Q}}_2^H \quad (24)$$

where $\mathbf{\Pi}_{\check{\mathbf{Q}}_1}^\perp \triangleq \mathbf{I}_{2M+1} - \check{\mathbf{Q}}_1(\check{\mathbf{Q}}_1^H\check{\mathbf{Q}}_1)^{-1}\check{\mathbf{Q}}_1^H$. Hence by substituting (24) into (20), we can obtain the oblique projection operator $\mathbf{E}_{\mathcal{A}_f|\mathcal{A}_n}$ as (cf. [49])

$$\mathbf{E}_{\mathcal{A}_f|\mathcal{A}_n} = \mathbf{A}_f(\check{\mathbf{Q}}_2\check{\mathbf{Q}}_2^H\mathbf{A}_f)^\dagger. \quad (25)$$

Evidently $\mathbf{E}_{\mathcal{A}_f|\mathcal{A}_n}$ in (25) is not affected by the unknown projector $\mathbf{\Pi}_{\mathcal{A}_n}^\perp$ and can be calculated from $\tilde{\mathbf{R}}$ and \mathbf{A}_f with the accessible array data, where the computationally burdensome eigendecomposition is avoided as well.

C. DOA Estimation of NF Signals

Now we consider the DOA estimation of NF signals in a computationally efficient manner. From (11)–(13) and (20)–(21), by using $\mathbf{E}_{\mathcal{A}_f|\mathcal{A}_n}$ in (25) to isolate the NF signals from the FF signals, we get a new correlation matrix \mathbf{R}_n corresponding to the NF signals from \mathbf{R} in (7) as

$$\begin{aligned} \mathbf{R}_n &= (\mathbf{I}_{2M+1} - \mathbf{E}_{\mathcal{A}_f|\mathcal{A}_n})\tilde{\mathbf{R}}(\mathbf{I}_{2M+1} - \mathbf{E}_{\mathcal{A}_f|\mathcal{A}_n})^H \\ &= \mathbf{A}_n\mathbf{R}_{sn}\mathbf{A}_n^H \\ &= \sum_{k=K_1+1}^K r_{s_k}\mathbf{a}_n(\theta_k, r_k)\mathbf{a}_n^H(\theta_k, r_k) \end{aligned} \quad (26)$$

where its pq th element $(\mathbf{R}_n)_{pq}$ is given by

$$\begin{aligned} &(\mathbf{R}_n)_{pq} \\ &= \sum_{k=K_1+1}^K r_{s_k} e^{j(-(p-q)\psi_k + ((p-M-1)^2 - (q-M-1)^2)\phi_k)} \end{aligned} \quad (27)$$

for $p, q = 1, 2, \dots, 2M+1$. Clearly when $p - q \neq 0$ and $(p - M - 1)^2 - (q - M - 1)^2 = 0$ [19], the quadratic term with ϕ_k in (27) is eliminated, i.e., we have

$$(\mathbf{R}_n)_{p, 2M+2-p} = \sum_{k=K_1+1}^K r_{s_k} e^{-j2(M+1-p)\psi_k} \triangleq r_n(p) \quad (28)$$

with $q = 2M + 2 - p$ for $p = 1, 2, \dots, 2M + 1$. Clearly $\{r_n(p)\}$ can be interpreted as the received ‘‘signals’’ for a virtual array of $2M + 1$ sensors illuminated by K_2 ‘‘signals’’ $\{r_{s_k}\}$ with the angles $\{\psi_k\}$, which are parameterized by the DOA θ_k of the

NF signals $s_k(n)$. Inspired by the Vandermonde factorization of Toeplitz matrix [61], [62], from (28) and after some simple algebraic manipulations, we can form the $(M+1) \times (M+1)$ Toeplitz correlation matrix \mathbf{T}_n as (cf. [63])

$$\begin{aligned} \mathbf{T}_n &\triangleq \begin{bmatrix} r_n(M+1), & r_n(M), & \dots, & r_n(1) \\ r_n(M+2), & r_n(M+1), & \dots, & r_n(2) \\ \vdots & \vdots & \ddots & \vdots \\ r_n(2M+1), & r_n(2M), & \dots, & r_n(M+1) \end{bmatrix} \\ &= \sum_{k=K_1+1}^K r_{s_k}\bar{\mathbf{a}}_n(\theta_k)\bar{\mathbf{a}}_n^H(\theta_k) = \bar{\mathbf{A}}_n\mathbf{R}_{sn}\bar{\mathbf{A}}_n^H \end{aligned} \quad (29)$$

where $\bar{\mathbf{a}}_n(\theta_k) \triangleq [1, e^{j2\psi_k}, e^{j4\psi_k}, \dots, e^{j2M\psi_k}]^T$, and $\bar{\mathbf{A}}_n \triangleq [\bar{\mathbf{a}}_n(\theta_{K_1+1}), \bar{\mathbf{a}}_n(\theta_{K_1+2}), \dots, \bar{\mathbf{a}}_n(\theta_K)]$. Evidently the $(M+1) \times K_2$ matrix $\bar{\mathbf{A}}_n$ is a Vandermonde matrix with full rank.

Similarly by dividing \mathbf{T}_n as $\mathbf{T}_n = [\mathbf{T}_{n1}^T, \mathbf{T}_{n2}^T]^T$, where \mathbf{T}_{n1} and \mathbf{T}_{n2} are two submatrices consisting of its first K_2 or the last $M+1 - K_2$ rows, when the number of snapshots is finite, the DOAs $\{\theta_k\}_{k=K_1+1}^K$ of NF signals can be estimated by minimizing the following cost function

$$f_n(\theta) = \bar{\mathbf{a}}_n^H(\theta)\mathbf{\Pi}_{\hat{\mathbf{Q}}}\bar{\mathbf{a}}_n(\theta) \quad (30)$$

where

$$\begin{aligned} \mathbf{\Pi}_{\hat{\mathbf{Q}}} &= \hat{\mathbf{Q}}(\hat{\mathbf{Q}}^H\hat{\mathbf{Q}})^{-1}\hat{\mathbf{Q}}^H \\ &= \hat{\mathbf{Q}}(\mathbf{I}_{M+1-K_2} - \hat{\mathbf{P}}^H(\hat{\mathbf{P}}\hat{\mathbf{P}}^H + \mathbf{I}_{K_2})^{-1}\hat{\mathbf{P}})\hat{\mathbf{Q}}^H \end{aligned} \quad (31)$$

$$\hat{\mathbf{P}} = (\hat{\mathbf{T}}_{n1}\hat{\mathbf{T}}_{n1}^H)^{-1}\hat{\mathbf{T}}_{n1}\hat{\mathbf{T}}_{n2}^H \quad (32)$$

and $\hat{\mathbf{Q}} = [\hat{\mathbf{P}}^T, -\mathbf{I}_{M+1-K_2}]^T$.

D. Range Estimation of NF Signals

Here we consider the range estimation of NF signals and the association between the estimated ranges and DOAs. Firstly the array response vector $\mathbf{a}_n(\theta_k, r_k)$ in (6) corresponding to the NF signals can be reexpressed as

$$\mathbf{a}_n(\theta_k, r_k) = \mathbf{\Psi}(\theta_k)\bar{\mathbf{a}}_n(\theta_k, r_k) \quad (33)$$

where $\bar{\mathbf{a}}_n(\theta_k, r_k) \triangleq [e^{jM^2\phi_k}, e^{j(M-1)^2\phi_k}, \dots, e^{j\phi_k}, 1]^T$, $\mathbf{\Psi}(\theta_k) = [\mathbf{D}^T(\theta_k), (\bar{\mathbf{J}}_M\mathbf{D}^*(\theta_k))^T]^T$, $\bar{\mathbf{J}}_M \triangleq [\mathbf{J}_M, \mathbf{0}_{M \times 1}]$, and $\mathbf{D}(\theta_k) \triangleq \text{diag}(e^{-jM\psi_k}, e^{-j(M-1)\psi_k}, \dots, e^{-j\psi_k}, 1)$. Clearly the parameters ψ_k (i.e., θ_k) and ϕ_k (i.e., θ_k and r_k) are decoupled in (33), and the dimension of $\bar{\mathbf{a}}_n(\theta_k, r_k)$ is smaller than that of $\mathbf{a}_n(\theta_k, r_k)$.

Hence as discussed above, in the case of finite number of snapshots, by using the estimated DOAs $\{\hat{\theta}_k\}_{k=K_1+1}^K$ of NF signals, from (15) and (33), the ranges $\{r_k\}_{k=K_1+1}^K$ of NF signals can be easily estimated by minimizing the following cost function

$$f_n(\hat{\theta}_k, r) = \bar{\mathbf{a}}_n^H(\hat{\theta}_k, r)\mathbf{\Psi}^H(\hat{\theta}_k)\mathbf{\Pi}_{\hat{\mathbf{Q}}}\mathbf{\Psi}(\hat{\theta}_k)\bar{\mathbf{a}}_n(\hat{\theta}_k, r) \quad (34)$$

where $\mathbf{\Pi}_{\hat{\mathbf{Q}}}$ is given by (18). Obviously the estimated ranges $\{\hat{r}_k\}_{k=K_1+1}^K$ and DOAs $\{\hat{\theta}_k\}_{k=K_1+1}^K$ are automatically paired without any additional processing, and the ranges are estimated more computationally efficient by employing $\bar{\mathbf{a}}_n(\theta_k, r_k)$ in (33) than $\mathbf{a}_n(\theta_k, r_k)$ in (6).

E. Measure Against Impact of Finite Data

In practice, the array covariance matrix \mathbf{R} should be estimated from finite array data. When the number of snapshots N is not sufficiently large enough, the nonzero residual cross-correlations between the incident signals and that between the incident signals and the additive noises result in the inaccurate estimate $\hat{\mathbf{R}}$ in (16) give by

$$\hat{\mathbf{R}} = \mathbf{A}\hat{\mathbf{R}}_s\mathbf{A}^H + \mathbf{A}\hat{\mathbf{R}}_{sw} + \hat{\mathbf{R}}_{sw}^H\mathbf{A}^H + \hat{\mathbf{R}}_w \quad (35)$$

where $\hat{\mathbf{R}}_{sw} = (1/N) \sum_{n=1}^N \mathbf{s}(n)\mathbf{w}^H(n)$. As a result, from (13) and (22), the estimate of $\hat{\mathbf{R}}$ in (22) can be expressed

$$\hat{\mathbf{R}} = \mathbf{A}_n\hat{\mathbf{R}}_{sn}\mathbf{A}_n^H\mathbf{\Pi}_{A_f}^\perp + \mathbf{A}_f\hat{\mathbf{R}}_{sfn}\mathbf{A}_n^H\mathbf{\Pi}_{A_f}^\perp + \Delta_w\mathbf{\Pi}_{A_f}^\perp \quad (36)$$

where $\hat{\mathbf{R}}_{sfn} = (1/N) \sum_{n=1}^N \mathbf{s}_f(n)\mathbf{s}_n^H(n)$, and

$$\Delta_w \triangleq \mathbf{A}\hat{\mathbf{R}}_{sw} + \hat{\mathbf{R}}_{sw}^H\mathbf{A}^H + \hat{\mathbf{R}}_w - \hat{\sigma}^2\mathbf{I}_{2M+1}. \quad (37)$$

Clearly when the number of snapshots is finite even though the SNR is high, the estimated signal covariance matrix $\hat{\mathbf{R}}_s$ is not strictly block diagonal, and the estimated cross-correlation matrix $\hat{\mathbf{R}}_{sfn} \neq \mathbf{O}_{K_1 \times K_2}$. Hence the range space of $\hat{\mathbf{R}}$ is not strictly equal to the range space of \mathbf{A}_n , and the estimated anti-diagonal elements $\{\hat{r}_n(p)\}$ in (28) also contain the information of FF signals. Consequently the residual cross-correlations $\hat{\mathbf{R}}_{sfn}$ will degrade the estimation accuracy of the oblique projection operator and hence the performance of DOA estimation of NF signals with (22), and the ‘‘saturation behavior’’ in the localization of NF signals will be encountered, where the estimation error doesn’t decrease with the increasing SNR. Similarly, when there are more than two NF signals present, the estimated anti-diagonal elements $\{\hat{r}_n(p)\}$ contain not only the DOA information but also the range information under the finite data case, and hence we will encounter another saturation problem.

Here we propose an alternating iterative scheme as a measure against the impact of finite array data. Firstly, we estimate the DOAs and ranges of NF signals with (30) and (34) and denote them as $\{\hat{\theta}_k^{(i)}\}_{k=K_1+1}^K$ and $\{\hat{r}_k^{(i)}\}_{k=K_1+1}^K$. Secondly, we divide the range space of the estimated array response matrix $\hat{\mathbf{A}}$ as

$$\mathcal{R}(\hat{\mathbf{A}}^{(i)}) = \mathcal{R}(\hat{\mathbf{a}}_{nk}) \oplus \mathcal{R}(\hat{\mathbf{A}}_k^{(i)}) \quad (38)$$

where $\hat{\mathbf{a}}_{nk}$ is the array response vector corresponding to the k th NF signal given by $\hat{\mathbf{a}}_{nk} = \mathbf{a}_n(\hat{\theta}_k^{(i)}, \hat{r}_k^{(i)})$, and $\hat{\mathbf{A}}_k^{(i)}$ denotes the array steering matrix without column $\hat{\mathbf{a}}_{nk}$ given by $\hat{\mathbf{A}}_k^{(i)} = [\mathbf{a}_f(\hat{\theta}_1), \mathbf{a}_f(\hat{\theta}_2), \dots, \mathbf{a}_f(\hat{\theta}_{K_1}), \mathbf{a}_n(\hat{\theta}_{K_1+1}^{(i)}, \hat{r}_{K_1+1}^{(i)}), \dots, \mathbf{a}_n(\hat{\theta}_{K_1+k-1}^{(i)}, \hat{r}_{K_1+k-1}^{(i)}), \mathbf{a}_n(\hat{\theta}_{K_1+k+1}^{(i)}, \hat{r}_{K_1+k+1}^{(i)}), \dots, \mathbf{a}_n(\hat{\theta}_K^{(i)}, \hat{r}_K^{(i)})]$. Then from (13), the estimated covariance matrix $\hat{\mathbf{R}}$ can be reexpressed as

$$\begin{aligned} \hat{\mathbf{R}} &= [\hat{\mathbf{a}}_{nk}, \hat{\mathbf{A}}_k^{(i)}] \begin{bmatrix} \hat{r}_{sk} & \hat{\boldsymbol{\rho}}^T \\ \hat{\boldsymbol{\rho}}^* & \hat{\mathbf{R}}_{Ak} \end{bmatrix} \begin{bmatrix} \hat{\mathbf{a}}_{nk}^H \\ (\hat{\mathbf{A}}_k^{(i)})^H \end{bmatrix} \\ &= \hat{r}_{sk}\hat{\mathbf{a}}_{nk}\hat{\mathbf{a}}_{nk}^H + \hat{\mathbf{a}}_{nk}\hat{\boldsymbol{\rho}}^T(\hat{\mathbf{A}}_k^{(i)})^H \\ &\quad + \hat{\mathbf{A}}_k^{(i)}\hat{\boldsymbol{\rho}}^*\mathbf{a}_{nk}^H + \hat{\mathbf{A}}_k^{(i)}\hat{\mathbf{R}}_{Ak}(\hat{\mathbf{A}}_k^{(i)})^H \end{aligned} \quad (39)$$

where $\hat{\boldsymbol{\rho}} = (1/N) \sum_{n=1}^N s_k(n)\mathbf{s}_{Ak}(n) \neq \mathbf{0}_{(K-1) \times 1}$, while $\mathbf{s}_{Ak}(n)$ and $\hat{\mathbf{R}}_{Ak}$ denote the signal vector without signal $s_k(n)$

and the sample signal covariance of $\mathbf{s}_{Ak}(n)$, respectively. Then in order to eliminate the second and third items in (39), we define a new oblique projection operator as

$$\hat{\mathbf{E}}_{\mathbf{A}_k|\mathbf{a}_{nk}}^{(i)} \triangleq \hat{\mathbf{A}}_k^{(i)} \left((\hat{\mathbf{A}}_k^{(i)})^H \mathbf{\Pi}_{\hat{\mathbf{a}}_{nk}}^\perp \hat{\mathbf{A}}_k^{(i)} \right)^{-1} (\hat{\mathbf{A}}_k^{(i)})^H \mathbf{\Pi}_{\hat{\mathbf{a}}_{nk}}^\perp \quad (40)$$

where $\mathbf{\Pi}_{\hat{\mathbf{a}}_{nk}}^\perp = \mathbf{I}_{2M+1} - \hat{\mathbf{a}}_{nk}(\hat{\mathbf{a}}_{nk}^H\hat{\mathbf{a}}_{nk})^{-1}\hat{\mathbf{a}}_{nk}^H$ for $k = K_1 + 1, K_1 + 2, \dots, K$. Thirdly, from (39) and (40), we get a new correlation matrix

$$\begin{aligned} \hat{\mathbf{R}}_{nk}^{(i)} &\triangleq (\mathbf{I}_{2M+1} - \hat{\mathbf{E}}_{\mathbf{A}_k|\mathbf{a}_{nk}}^{(i)})\hat{\mathbf{R}}(\mathbf{I}_{2M+1} - \hat{\mathbf{E}}_{\mathbf{A}_k|\mathbf{a}_{nk}}^{(i)})^H \\ &\approx \hat{r}_{sk}\hat{\mathbf{a}}_{nk}\hat{\mathbf{a}}_{nk}^H \end{aligned} \quad (41)$$

where $\hat{\mathbf{R}}_{nk}$ only contains the information of the k th NF signal. Hence the estimate of \mathbf{R}_n in (26) can be obtained as

$$\hat{\mathbf{R}}_n^{(i)} = \sum_{k=K_1+1}^K \hat{\mathbf{R}}_{nk}^{(i)}. \quad (42)$$

Finally, the DOAs and ranges of NF signals are estimated with (29), (30), and (34) from $\hat{\mathbf{R}}_n^{(i)}$ in (42) and denoted as $\{\hat{\theta}_k^{(i+1)}\}_{k=K_1+1}^K$ and $\{\hat{r}_k^{(i+1)}\}_{k=K_1+1}^K$, while the index is updated as $i = i + 1$. We can repeat this procedure several times until the difference between two consecutive iterations becomes smaller than a threshold, i.e.,

$$\sum_{k=K_1+1}^K \left| \hat{\theta}_k^{(i+1)} - \hat{\theta}_k^{(i)} \right| \leq \varepsilon \quad (43)$$

where ε is an arbitrary and positive small constant (e.g., $\varepsilon = 10^{-6}$), then we denote $\hat{\theta}_k = \hat{\theta}_k^{(i+1)}$.

F. Implementation of Proposed Method

As shown in Fig. 2, when the finite array data $\{\mathbf{x}(n)\}_{n=1}^N$ are available, the implementation of the proposed LOFNS method is summarized as follows:

- 1) Estimate the matrix $\hat{\mathbf{R}}$ from $\{\mathbf{x}(n)\}_{n=1}^N$ with (16). $\mathcal{O}[(2M+1)^2N]$ flops
- 2) Estimate the matrix $\hat{\mathbf{R}}$ from $\hat{\mathbf{R}}$ with (11)–(13). $\mathcal{O}[(2M+1)^3 + (2M+1)^2K + (2M+1)K^2]$ flops
- 3) Estimate the DOAs $\{\theta_k\}_{k=1}^{K_1}$ of FF signals from the phases of the K_1 zeros of the polynomial $p_f(z)$ closest to the unit circle in the z -plane with (18) and (19)
$$p_f(z) \triangleq z^{2M}\mathbf{g}_f^H(z)\mathbf{\Pi}_Q\mathbf{g}_f(z) \quad (44)$$

where $\mathbf{g}_f(z) \triangleq [z^M, \dots, z, 1, z^{-1}, \dots, z^{-M}]^T$, and $z \triangleq e^{j2\pi d \sin \theta / \lambda}$. $\mathcal{O}[(2M+1)^3 + (2M+1)^2K + (2M+1)K^2]$ flops
- 4) Estimate the oblique projection operator $\hat{\mathbf{E}}_{\mathbf{A}_f|\mathbf{A}_n}$ from $\hat{\mathbf{R}}$ and $\{\hat{\theta}_k\}_{k=1}^{K_1}$ with (22)–(25). $\mathcal{O}[(2M+1)^3 + (2M+1)^2K_1 + (2M+1)K_1^2]$ flops
- 5) Estimate the matrix $\hat{\mathbf{R}}_n$ from $\hat{\mathbf{R}}$ and $\hat{\mathbf{E}}_{\mathbf{A}_f|\mathbf{A}_n}$ with (26), and form the matrix $\hat{\mathbf{T}}_n$ from the anti-diagonal elements $\{\hat{r}_n(p)\}$ of $\hat{\mathbf{R}}_n$ with (29). $\mathcal{O}[(2M+1)^3]$ flops
- 6) Estimate the DOAs $\{\theta_k\}_{k=K_1+1}^K$ of NF signals from the phases of the K_2 zeros of the polynomial $p_n(z)$ closest to

the unit circle in the z -plane with (31) and (32)

$$p_n(z) \triangleq z^{M+1} \mathbf{g}_n^H(z) \mathbf{\Pi}_{\hat{Q}} \mathbf{g}_n(z) \quad (45)$$

where $\mathbf{g}_n(z) \triangleq [1, z^{-1}, \dots, z^{-M}]^T$ and $z \triangleq e^{j4\pi d \sin \theta / \lambda}$, and denote these estimates as $\{\hat{\theta}_k^{(i)}\}_{k=K_1+1}^K$, where $i = 0$.

$\mathcal{O}[(M+1)^3 + (M+1)^2 K_2 + (M+1) K_2^2]$ flops

- 7) Estimate the ranges $\{r_k\}_{k=K_1+1}^K$ of NF signals from the phases of the K_2 zeros of the polynomial $\bar{p}_n(z)$ closest to the unit circle in the z -plane with $\{\hat{\theta}_k\}_{k=K_1+1}^K$ and (18), (19), and (34)

$$\bar{p}_n(z) \triangleq z^{M^2} \bar{\mathbf{g}}_n^H(z) \mathbf{\Psi}^H(\hat{\theta}_k) \mathbf{\Pi}_{\hat{Q}} \mathbf{\Psi}(\hat{\theta}_k) \bar{\mathbf{g}}_n(z) \quad (46)$$

where $\bar{\mathbf{g}}_n(z) \triangleq [1, z, \dots, z^{(M-1)^2}, z^{M^2}]^T$, and $z \triangleq e^{j\pi d^2 \cos^2 \theta / (\lambda r)}$.

$$\mathcal{O}[K_2((M+1)^3 + (M+1)^2 M + (M+1) M^2)] \text{ flops}$$

- 8) Estimate the matrix $\hat{\mathbf{R}}_n^{(i)}$ from $\{\hat{\theta}_k\}_{k=1}^{K_1}$, $\{\hat{\theta}_k^{(i)}\}_{k=K_1+1}^K$ and $\{\hat{r}_k^{(i)}\}_{k=K_1+1}^K$ with (40)–(42), and repeat Steps 6 and 7 to estimate the DOAs and ranges of NF signals again and denote them as $\{\hat{\theta}_k^{(i+1)}\}_{k=K_1+1}^K$ and $\{\hat{r}_k^{(i+1)}\}_{k=K_1+1}^K$.

$$\mathcal{O}[K_2((2M+1)^3 + (2M+1)^2 K + (2M+1) K^2)] \text{ flops}$$

- 9) If the condition in (43) is not satisfied, repeat Step 8 by setting $i = i + 1$; otherwise, reexpress $\{\hat{\theta}_k^{(i+1)}\}_{k=K_1+1}^K$ and $\{\hat{r}_k^{(i+1)}\}_{k=K_1+1}^K$ as the final estimates $\{\hat{\theta}_k\}_{k=K_1+1}^K$ and $\{\hat{r}_k\}_{k=K_1+1}^K$.

The computational complexity of each step is roughly indicated in terms of the number of flops, where one flop is defined as a floating-point addition or multiplication operation as adopted by MATLAB software, and the computational complexity of LOFNS is nearly in order of $\mathcal{O}[(2M+1)^2 N + (2M+1)^3]$ flops, when $2M+1 \gg K$, which occurs often in practical applications of localization, and a few times of the alternating iterations is required and set at 3 through the empirical examples.

Remark D: The implementation of the GESPR [39] involves the computation of array covariance matrix and its eigendecomposition, and the rooting of two MUSIC-like polynomials for DOA and range estimation, while that of the OPMUSIC [41] involves the computations of array covariance matrix and the projected array covariance matrix and their eigendecompositions, and three peak picking procedures of the MUSIC-like spectra. Hence the major computational complexities of the GESPR and the OPMUSIC are approximately in order of $\mathcal{O}[(2M+1)^2 N + (2M+1)^2 + (2M+1) K^2]$ and $\mathcal{O}[(2M+1)^2 N + (2M+1)^3 + (180/\Delta\theta)(2M+1)^2 + ((2D^2/\lambda) - 0.62(D^3/\lambda)^{1/2}/\Delta r)(2M+1)^2]$ [39], respectively, where $\Delta\theta$ and Δr denote the angular grid of spectrum searching and the range grid of spectrum searching. Fig. 3 shows the quantitative comparisons between the proposed LOFNS with the GESPR and the OPMUSIC in MATLAB flops versus the number of snapshots and the number of sensors. It is clear that the LOFNS is computationally more efficient than these existing methods [39], [41], since the computationally burdensome eigendecomposition procedure and peak searching are avoided. ■

Remark E: We previously proposed a subspace-based method (i.e., SUMWE) for the coherent narrowband FF signals

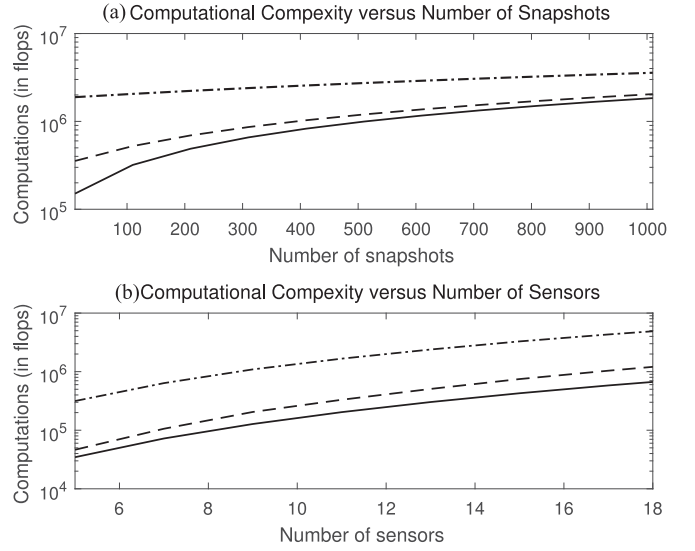


Fig. 3. Comparison of computational complexities in MATLAB flops versus (a) the number of the snapshots ($2M+1=13$) and (b) the number of the sensors ($N=200$) (dashed line: GESPR; dash-dotted line: OPMUSIC; solid line: the proposed LOFNS w/o iteration; $\Delta\theta = 0.02^\circ$ and $\Delta r = 0.02\lambda$).

impinging on the ULA [11], where the coherency of incident signals is decorrelated through subarray averaging, and the null space can be obtained through a linear operation from a Hankel matrix formed from the cross-correlations between some sensor data. Although the basic idea of linear operator (cf. [10]) is also utilized to avoid computationally burdensome eigendecomposition, the SUMWE is only suitable for the coherent FF signals owing to the reduced effective aperture of array/subarray. ■

IV. STATISTICAL ANALYSIS

When the number of snapshots is sufficiently large, herein we analyze the asymptotic properties of the estimated DOAs of FF signals and the estimated DOAs and ranges of NF signals by using the proposed LOFNS, where the analytical expressions of the asymptotic MSEs are clarified.

A. Asymptotic Properties for FF Signals

Firstly we consider the consistency of the DOA estimates for the FF signals, and we easily have the following lemma.

Lemma 1: As the number of snapshots N tends to infinity, the estimates $\{\hat{\theta}_k\}_{k=1}^{K_1}$ of FF signals obtained by minimizing the cost function $f(\theta)$ in (17) approach the true parameters $\{\theta\}_{k=1}^{K_1}$ with probability one (w.p.1).

Proof: This lemma can be readily established by adopting the proof of similar Lemma in [11], [64], [65]. ■

From this lemma, we have the asymptotic MSE expression of the estimated DOAs $\{\hat{\theta}_k\}_{k=1}^{K_1}$ of FF signals as follows.

Theorem 1: The large-sample MSE of the estimation error $\hat{\theta}_k - \theta_k$ of FF signals obtained by (17) is given by

$$\begin{aligned} \text{MSE}(\hat{\theta}_k) &= \text{var}\{\hat{\theta}_k\} \\ &= \frac{1}{2N H_{fkk}^2} \text{Re}\{\text{vec}(\mathbf{R})^H (\mathbf{M}_k^* \otimes \mathbf{M}_k) \text{vec}(\mathbf{R})\} \quad (47) \end{aligned}$$

where $\mathbf{M}_k \triangleq \mathbf{h}_f(\theta_k) \mathbf{g}_f^H(\theta_k)$, $\mathbf{g}_f(\theta_k) \triangleq \mathbf{\Pi}_Q \mathbf{d}_f(\theta_k)$, $\mathbf{h}_f(\theta_k) \triangleq \bar{\mathbf{R}}_1^H (\bar{\mathbf{R}}_1 \bar{\mathbf{R}}_1^H)^{-1} \mathbf{a}_{f1}(\theta_k)$, $H_{fkk} \triangleq \mathbf{d}_f^H(\theta_k) \mathbf{\Pi}_Q \mathbf{d}_f(\theta_k)$, $\mathbf{d}_f(\theta_k)$

$\triangleq d(\mathbf{a}_f(\theta))/d\theta|_{\theta=\theta_k}$, and $\mathbf{a}_{f1}(\theta_k)$ denotes the k th column of \mathbf{A}_1 .

Proof: See Appendix A. ■

B. Asymptotic Properties for NF Signals

Since the localization of NF signals requires the oblique projection operator with the knowledge of the FF signals, the statistical analysis of the estimation performance of NF signals is more difficult and complicated. Herein for facilitating the statistical analysis, we study the large-sample MSEs of the estimated DOAs and ranges of NF signals with true values of the oblique protection operators in (40).

Lemma 2: As the number of snapshots N tends to infinity, the estimates $\{\hat{\theta}\}_{k=K_1+1}^K$ of NF signals obtained by minimizing the cost function $f_n(\theta)$ in (30) approach the true parameters $\{\theta\}_{k=K_1+1}^K$ w.p.1.

Proof: This lemma can be readily established by adopting the proof of Lemma in [65]. ■

Then from this lemma, we get the asymptotic MSE expression of the estimates $\{\hat{\theta}_k\}_{k=K_1+1}^K$ of NF signals as follows.

Theorem 2: The large-sample MSE of the estimates $\{\hat{\theta}_k\}_{k=K_1+1}^K$ of NF signals obtained by (30) is given by

$$\begin{aligned} \text{MSE}(\hat{\theta}_k) &= \text{var}\{\hat{\theta}_k\} \\ &= \frac{1}{2NH_{nkk}^2} \text{Re}\left\{ \text{tr}\{(\bar{\mathbf{M}}_k \mathbf{R})^2\} + \xi_k^2 \text{tr}\{(\mathbf{M} \mathbf{R})^2\} \right. \\ &\quad + \text{vec}(\mathbf{R})^H (\bar{\mathbf{M}}_k^* \otimes \bar{\mathbf{M}}_k) \text{vec}(\mathbf{R}) \\ &\quad + \xi_k^2 \text{vec}(\mathbf{R})^H (\mathbf{M}^* \otimes \mathbf{M}) \text{vec}(\mathbf{R}) \\ &\quad - 2\xi_k \left(\text{vec}(\mathbf{R})^H (\mathbf{M}^* \otimes \bar{\mathbf{M}}_k) \text{vec}(\mathbf{R}) \right. \\ &\quad \left. \left. + \text{vec}^H(\mathbf{R})(\bar{\mathbf{M}}_k^T \otimes \mathbf{M}) \text{vec}(\mathbf{R}) \right) \right\} \quad (48) \end{aligned}$$

where $\bar{\mathbf{M}}_k \triangleq (\mathbf{g}_n^H(\theta_k) \otimes \mathbf{I}_{2M+1}) \mathbf{C}(\mathbf{h}_n(\theta_k) \otimes \mathbf{I}_{2M+1})$, $\mathbf{M} \triangleq \text{blkdiag}(\mathbf{O}_{K \times K}, \mathbf{\Pi})$, $\mathbf{g}_n(\theta_k) \triangleq \mathbf{\Pi}_Q \mathbf{d}_n(\theta_k)$, $\mathbf{h}_n(\theta_k) \triangleq \mathbf{T}_{n1}^H \cdot (\mathbf{T}_{n1} \mathbf{T}_{n1}^H)^{-1} \bar{\mathbf{a}}_{n1}(\theta_k)$, $H_{nkk} \triangleq \mathbf{d}_n^H(\theta_k) \mathbf{\Pi}_Q \mathbf{d}_n(\theta_k)$, $\mathbf{d}_n(\theta_k) \triangleq d\bar{\mathbf{a}}_n(\theta)/(d\theta)|_{\theta=\theta_k}$, $\xi_k \triangleq \text{Re}\{\mathbf{g}_n^H(\theta_k) \tilde{\mathbf{B}} \mathbf{h}_n(\theta_k)\}/(2M+1-2K)$, and

$$\tilde{\mathbf{B}} = \sum_{k=K_1+1}^K \tilde{\mathbf{B}}_k, \quad \mathbf{C} = \sum_{k=K_1+1}^K \mathbf{C}_k \quad (49)$$

$$\mathbf{B}_k \triangleq \mathbf{I} - \mathbf{E}_{\mathbf{A}_k | \mathbf{a}_{nk}} = [\mathbf{b}_{-M}^{(k)}, \dots, \mathbf{b}_0^{(k)}, \dots, \mathbf{b}_M^{(k)}]^T \quad (50)$$

$$\tilde{\mathbf{B}}_k \triangleq \begin{bmatrix} \mathbf{b}_0^{(k)T} \mathbf{b}_0^{(k)*} & \mathbf{b}_{-1}^{(k)T} \mathbf{b}_1^{(k)*} & \dots & \mathbf{b}_{-M}^{(k)T} \mathbf{b}_M^{(k)*} \\ \mathbf{b}_1^{(k)T} \mathbf{b}_{-1}^{(k)*} & \mathbf{b}_0^{(k)T} \mathbf{b}_0^{(k)*} & \dots & \mathbf{b}_{-M+1}^{(k)T} \mathbf{b}_{M-1}^{(k)*} \\ \vdots & \vdots & \ddots & \vdots \\ \mathbf{b}_M^{(k)T} \mathbf{b}_{-M}^{(k)*} & \mathbf{b}_{M-1}^{(k)T} \mathbf{b}_{-M+1}^{(k)*} & \dots & \mathbf{b}_0^{(k)T} \mathbf{b}_0^{(k)*} \end{bmatrix} \quad (51)$$

$$\mathbf{C}_k \triangleq \begin{bmatrix} \mathbf{b}_0^{(k)*} \mathbf{b}_0^{(k)T} & \mathbf{b}_1^{(k)*} \mathbf{b}_{-1}^{(k)T} & \dots & \mathbf{b}_M^{(k)*} \mathbf{b}_{-M}^{(k)T} \\ \mathbf{b}_{-1}^{(k)*} \mathbf{b}_1^{(k)T} & \mathbf{b}_0^{(k)*} \mathbf{b}_0^{(k)T} & \dots & \mathbf{b}_{M-1}^{(k)*} \mathbf{b}_{-M+1}^{(k)T} \\ \vdots & \vdots & \ddots & \vdots \\ \mathbf{b}_{-M}^{(k)*} \mathbf{b}_M^{(k)T} & \mathbf{b}_{-M+1}^{(k)*} \mathbf{b}_{M-1}^{(k)T} & \dots & \mathbf{b}_0^{(k)*} \mathbf{b}_0^{(k)T} \end{bmatrix} \quad (52)$$

while $\bar{\mathbf{a}}_{n1}$ denotes the $(k-K_1)$ th column of $\bar{\mathbf{A}}_{n1}$, which consists of the first K_2 rows of $\bar{\mathbf{A}}_n$ in (29).

Proof: See Appendix B. ■

Similarly as studied in Section IV-A, we easily obtain the large-sample MSE of estimated ranges of NF signals.

Theorem 3: The large-sample MSE of the estimates $\{\hat{r}_k\}_{k=K_1+1}^K$ of NF signals obtained by (34) is given by

$$\begin{aligned} \text{MSE}(\hat{r}_k) &= \text{var}\{\hat{r}_k\} \\ &= \frac{1}{2NH_{rkk}^2} \text{Re}\{\text{vec}(\mathbf{R})^H (\tilde{\mathbf{M}}_k^* \otimes \tilde{\mathbf{M}}_k) \text{vec}(\mathbf{R})\} \quad (53) \end{aligned}$$

where $\tilde{\mathbf{M}}_k \triangleq \mathbf{h}_n(r_k) \mathbf{g}_n^H(r_k)$, $\mathbf{g}_n(r_k) \triangleq \mathbf{\Pi}_Q \mathbf{d}_n(r_k)$, $\mathbf{h}_n(r_k) \triangleq \bar{\mathbf{R}}_1^H (\bar{\mathbf{R}}_1 \bar{\mathbf{R}}_1^H)^{-1} \mathbf{a}_{n1}(r_k)$, $H_{rkk} \triangleq \mathbf{d}_n^H(r_k) \mathbf{\Pi}_Q \mathbf{d}_n(r_k)$, $\mathbf{d}_n(r_k) \triangleq d(\mathbf{a}_n(\theta_k, r))/dr|_{r=r_k}$, and $\mathbf{a}_{n1}(\theta_k)$ denotes the k th column of \mathbf{A}_1 .

Proof: The proof of this Theorem is same to that of the Theorem 1 (see Appendix A for details). ■

C. Analytic Study of Performance

As the general expressions of asymptotic MSEs derived above are much complicated, now we specialize in the case of two signal with equal power (i.e., one FF signal and one NF signal) for gaining insights into the proposed LOFNS.

In this case (i.e., $K_1 = K_2 = 1$), we readily obtain

$$\mathbf{A}_f = \mathbf{a}_f(\theta_1), \quad \mathbf{A}_n = \mathbf{a}_n(\theta_2, r_2), \quad \bar{\mathbf{A}}_n = \bar{\mathbf{a}}_n(\theta_2) \quad (54)$$

$$\mathbf{R}_s = r_s \mathbf{I}_2, \quad \mathbf{T}_{n1} = r_s \bar{\mathbf{a}}_n(\theta_2) \quad (55)$$

where $\mathbf{a}_f^H(\theta_1) \mathbf{a}_f(\theta_1) = 2M+1$, $\mathbf{a}_n^H(\theta_2, r_2) \mathbf{a}_n(\theta_2, r_2) = 2M+1$, $\bar{\mathbf{a}}_n^H(\theta_2) \bar{\mathbf{a}}_n(\theta_2) = M+1$, and $\mathbf{h}_n(\theta_2) = \bar{\mathbf{a}}_n(\theta_2)/(M+1)r_s$, and by performing some manipulations, we get $\text{tr}\{\mathbf{M} \mathbf{R}\} = \sigma^2(2M+1-2K)$, $\text{tr}\{(\mathbf{M} \mathbf{R})^2\} = \sigma^4(2M+1-2K)$, $\mathbf{A}^H \bar{\mathbf{M}}_k \mathbf{A} = \mathbf{O}_{K \times K}$, $\mathbf{M} \bar{\mathbf{R}} = \mathbf{O}_{(2M+1) \times (2M+1)}$, and

$$\begin{aligned} \text{tr}\{\bar{\mathbf{M}}_k\} &= \sum_{i=1}^{2M+1} \mathbf{g}_n^H(\theta_k) (\mathbf{I}_{M+1} \otimes \mathbf{e}_i^T) \mathbf{C}(\mathbf{I}_{M+1} \otimes \mathbf{e}_i) \mathbf{h}_n(\theta_k) \\ &= \mathbf{g}_n^H(\theta_k) \tilde{\mathbf{B}} \mathbf{h}_n(\theta_k). \quad (56) \end{aligned}$$

Further by using the fact that

$$\text{vec}^H(\mathbf{C})(\mathbf{A}^T \otimes \mathbf{B}) \text{vec}(\mathbf{C}) = \text{tr}\{\mathbf{A} \mathbf{C} \mathbf{B} \mathbf{C}\} \quad (57)$$

from (47), we have

$$\begin{aligned} \text{vec}(\mathbf{R})^H (\mathbf{M}_1^* \otimes \mathbf{M}_1) \text{vec}(\mathbf{R}) &= \text{tr}\{\mathbf{M}_1^H \mathbf{R} \mathbf{M}_1 \mathbf{R}\} \\ &= \text{tr}\{(\mathbf{M}_1^H \bar{\mathbf{R}} + \sigma^2 \mathbf{M}_1^H)(\mathbf{M}_1 \bar{\mathbf{R}} + \sigma^2 \mathbf{M}_1)\} \\ &= \sigma^4 \text{tr}\{\mathbf{M}_1^H \mathbf{M}_1\} \\ &= \sigma^4 \text{tr}\{\mathbf{g}_f(\theta_1) \mathbf{h}_f^H(\theta_1) \mathbf{R} \mathbf{h}_f(\theta_1) \mathbf{g}_f^H(\theta_1) \mathbf{R}\} \\ &= \sigma^4 \mathbf{h}_f^H(\theta_1) \mathbf{R} \mathbf{h}_f(\theta_1) \mathbf{g}_f^H(\theta_1) \mathbf{R} \mathbf{g}_f(\theta_1) \quad (58) \end{aligned}$$

where

$$\begin{aligned} \mathbf{g}_f^H(\theta_1) \mathbf{R} \mathbf{g}_f(\theta_1) &= \mathbf{d}_f^H(\theta_1) \mathbf{\Pi}_Q \mathbf{R} \mathbf{\Pi}_Q \mathbf{d}_f(\theta_1) \\ &= \mathbf{d}_f^H(\theta_1) \mathbf{\Pi}_Q (\bar{\mathbf{R}} + \sigma^2 \mathbf{I}_{2M+1}) \mathbf{\Pi}_Q \mathbf{d}_f(\theta_1) \\ &= 0 + \sigma^2 H_{f11} \end{aligned} \quad (59)$$

and

$$\begin{aligned} \mathbf{h}_f^H(\theta_1) \mathbf{R} \mathbf{h}_f(\theta_1) &= \mathbf{a}_{f1}^H (\bar{\mathbf{R}}_1 \bar{\mathbf{R}}_1^H)^{-1} \bar{\mathbf{R}}_1 (\mathbf{A} \mathbf{R}_s \mathbf{A}^H + \sigma^2 \mathbf{I}_{2M+1}) \\ &\quad \cdot \bar{\mathbf{R}}_1 (\bar{\mathbf{R}}_1 \bar{\mathbf{R}}_1^H)^{-1} \mathbf{a}_{f1} \\ &= \mathbf{a}_{f1}^H (\mathbf{A}_1 \mathbf{R}_s \mathbf{A}^H \mathbf{A} \mathbf{R}_s \mathbf{A}_1^H)^{-1} \mathbf{A}_1 \mathbf{R}_s \mathbf{A}^H (\mathbf{A} \mathbf{R}_s \mathbf{A}^H \\ &\quad + \sigma^2 \mathbf{I}_{2M+1}) \mathbf{A}_1 \mathbf{R}_s \mathbf{A}^H (\mathbf{A}_1 \mathbf{R}_s \mathbf{A}^H \mathbf{A} \mathbf{R}_s \mathbf{A}_1^H)^{-1} \mathbf{a}_{f1} \\ &= \mathbf{a}_{f1}^H \mathbf{A}_1^{-H} \mathbf{R}_s^{-1} (\mathbf{A}^H \mathbf{A})^{-1} \mathbf{A}^H (\mathbf{A} \mathbf{R}_s \mathbf{A}^H \\ &\quad + \sigma^2 \mathbf{I}_{2M+1}) \mathbf{A} (\mathbf{A}^H \mathbf{A})^{-1} \mathbf{R}_s^{-1} \mathbf{A}_1^{-1} \mathbf{a}_{f1} \\ &= \mathbf{a}_{f1}^H \mathbf{A}_1^{-H} (\mathbf{R}_s^{-1} + \sigma^2 \mathbf{R}_s^{-1} (\mathbf{A}^H \mathbf{A})^{-1} \mathbf{R}_s^{-1}) \mathbf{A}_1^{-1} \mathbf{a}_{f1} \\ &= \frac{2M+1}{(2M+1)^2 - |\mathbf{a}_f^H(\theta_1) \mathbf{a}_n(\theta_2, r_2)|^2} \triangleq \alpha \end{aligned} \quad (60)$$

where $\bar{\mathbf{R}}_1 = \mathbf{A}_1 \mathbf{R}_s \mathbf{A}^H$ is used. Then by substituting (58)–(60) into (47), from Theorems 1, we can obtain the asymptotic MSE of the estimated DOA of the FF signal

$$\text{MSE}(\hat{\theta}_1) = \frac{1}{2N} \frac{1}{\text{SNR}} \frac{1}{H_{f11}} \left(1 + \frac{\alpha}{\text{SNR}} \right) \quad (61)$$

Additionally by performing some similar manipulations, from Theorems 2 and 3, we can obtain the asymptotic MSEs of the estimated location parameters of the NF signal

$$\text{MSE}(\hat{\theta}_2) = \frac{1}{2N} \frac{1}{(M+1)^2} \frac{1}{\text{SNR}} \frac{1}{H_{n22}^2} \left(\beta + \frac{\gamma}{\text{SNR}} \right) \quad (62)$$

$$\text{MSE}(\hat{r}_2) = \frac{1}{2N} \frac{1}{\text{SNR}} \frac{1}{H_{r22}} \left(1 + \frac{\alpha}{\text{SNR}} \right) \quad (63)$$

where $\text{SNR} \triangleq r_s/\sigma^2$, and

$$\beta \triangleq \text{Re} \left\{ 2\text{tr}\{\mathbf{F} \mathbf{U} \mathbf{F}\} + \text{tr}\{\mathbf{F}^H \mathbf{U} \mathbf{F}\} + \text{tr}\{\mathbf{F} \mathbf{U} \mathbf{F}^H\} \right\} \quad (64)$$

$$\begin{aligned} \gamma \triangleq & \text{Re} \left\{ \text{tr}\{\mathbf{F} \mathbf{F}\} + \text{tr}\{\mathbf{F}^H \mathbf{F}\} + \frac{2\text{Re}\{\text{tr}\{\mathbf{F}\}\}}{2M+1-2K} \right. \\ & \left. \cdot (\text{Re}\{\text{tr}\{\mathbf{F}\}\} - 2\text{tr}\{\mathbf{F} \mathbf{M}\}) \right\} \end{aligned} \quad (65)$$

$$\mathbf{F} \triangleq (\mathbf{g}_n^H(\theta_2) \otimes \mathbf{I}_{2M+1}) \mathbf{C}(\bar{\mathbf{a}}(\theta_2) \otimes \mathbf{I}_{2M+1}) \quad (66)$$

while $\mathbf{U} = (2M+1) \mathbf{A} \mathbf{A}^H$, and $\mathbf{A} = [\mathbf{a}_f(\theta_1), \mathbf{a}_n(\theta_2, r_2)]$.

Hence from (61)–(63), we can find that the asymptotic MSEs of the estimated DOAs and range decrease monotonically with increasing the number of snapshots N or SNR, which means the LOFNS estimator is asymptotically efficient (for large N). Further, we can see that the estimated DOA of the NF signal has smaller estimation error than that of the FF signals, i.e., $\text{MSE}(\hat{\theta}_2) < \text{MSE}(\hat{\theta}_1)$ for large number of sensors and SNR, when the number of snapshots N is finite.

V. NUMERICAL EXAMPLES

Now we evaluate the estimation performance of the proposed LOFNS through several numerical examples, where some existing localization methods of the mixed FF and NF signals with eigendecomposition such as the method of passive localization (MPL) [36], the spatial differencing method (SDM) [38], the GESPR [39], the OPMUSIC [41], and the OPMUGE [43] are carried out for performance comparison, and the stochastic Cramer-Rao lower bound (CRB) [41] is also calculated. Additionally one RMT-based direction method (i.e., the G-MUSIC) [55] is also modified and implemented for estimating the location parameters of the FF and NF signals, where the cost function is replaced by the MUSIC-like cost functions used in the OPMUSIC [41], because the existing RMT-based methods were developed for the DOA estimation of the FF signals. The results are all based on 1000 independent trials.

Example 1–Performance versus SNR: There are four FF and NF signals with equal power arriving from the locations $(-43^\circ, \infty)$, $(-20^\circ, \infty)$, $(17^\circ, 3.0\lambda)$, and $(54^\circ, 4.4\lambda)$, and the symmetrical ULA has 13-sensors (i.e., $M = 6$) with element spacing $d = \lambda/4$. The SNR is varied from -10 dB to 40 dB, and the number of snapshots is fixed at $N = 200$.

The averaged root-MSEs (RMSEs) of the estimated DOA $\hat{\theta}_1$ of one FF signal, the estimated DOA $\hat{\theta}_3$ of one NF signal and the estimated ranges \hat{r}_3, \hat{r}_4 of NF signals in terms of the SNR are plotted in Figs. 4 and 5, individually. Obviously the LOFNS performs well as the existing methods with eigendecomposition such as the methods [36], [38], [41], and [43] and outperforms [39] for the DOA estimation of FF signal. Unfortunately, the nonzero residual cross-correlations between the incident signals and that between the incident signals and the additive noises due to the finite array data result in the inaccurate structure of sample covariance matrix of incident signals or oblique projection operator. As a result, the MPL [36], the SDM [38], the OPMUSIC [41], and the OPMUGE [43] and the LOFNS without alternating iterative scheme suffer from serious “saturation behaviors” in the localization of NF signals even at high SNRs, where the estimated DOAs and ranges have high elevated error floors, and they do not decrease monotonically with the increasing SNR. Meanwhile the GESPR [39] also has rather large errors in the parameter estimation of NF signals due to the GESPRIT as mentioned in Section I. In addition, the G-MUSIC [55] performs similarly as the OPMUSIC [41], and it suffers from “saturation behaviors” in the DOA and range estimation of the NF signals, too. However, by using the LOFNS with alternating iterative scheme, the localization performance of NF signals is improved dramatically in the high SNR region, though the number of snapshots is finite. Furthermore, we can find that the empirical RMSEs of the LOFNS are very close to the theoretical ones (except at low SNR) and the difference between the theoretical RMSEs and the CRBs [41] is small, and the theoretical and empirical RMSEs of the LOFNS decrease monotonically with the increasing SNR, while the theoretical RMSE of the estimated DOA of the NF signal is slightly smaller than that of the FF signal at medium to higher SNRs as clarified in Section IV.

Example 2–Performance versus Number of Snapshots: The simulation conditions are similar to those in Example 1, except that the number of snapshots is varied from 16 to 10000, and the SNR is fixed at 10 dB. The averaged RMSEs of the estimates

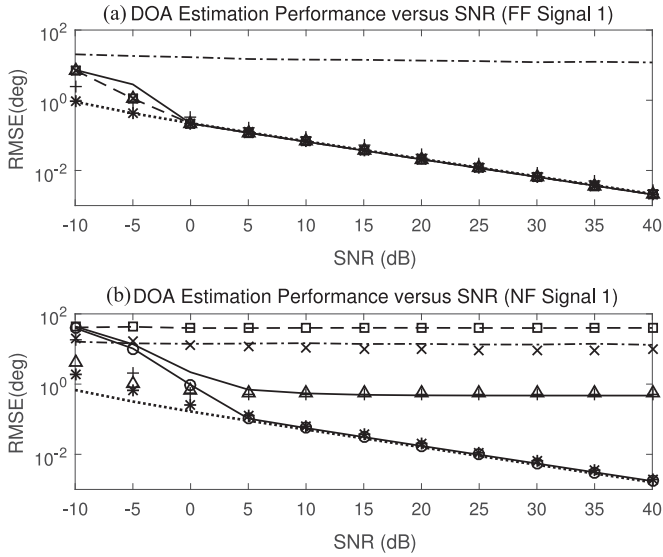


Fig. 4. The RMSEs of the estimated DOAs for (a) the FF signal and (b) the NF signal versus the SNR (dashed line: MPL; “x”: SDM; dash-dotted line: GESPR; “ Δ ”: OPMUSIC; “ \square ”: OPMUGE; “+”: G-MUSIC; solid line: LOFNS w/o iteration; solid line with “o”: LOFNS; “*”: theoretical RMSE of LOFNS; and dotted line: CRB) for Example 1.

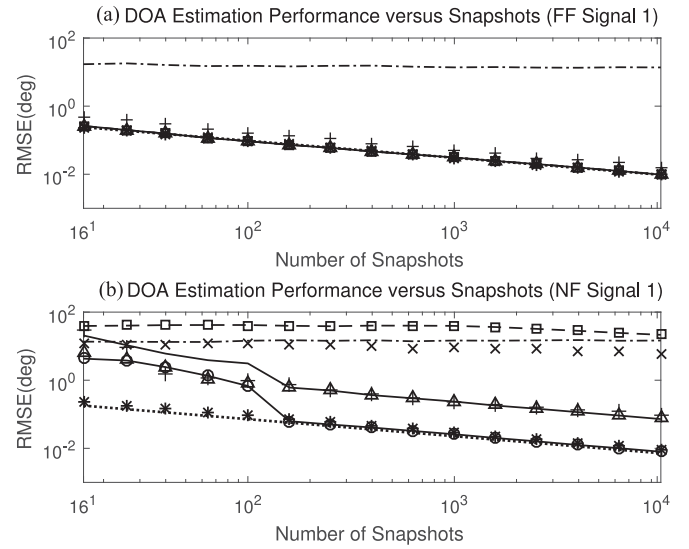


Fig. 6. The RMSEs of the estimated DOAs of (a) FF and (b) NF signals versus the number of snapshots (dashed line: MPL; “x”: SDM; dash-dotted line: GESPR; “ Δ ”: OPMUSIC; “ \square ”: OPMUGE; “+”: G-MUSIC; solid line: LOFNS w/o iteration; solid line with “o”: LOFNS; “*”: theoretical RMSE of LOFNS; and dotted line: CRB) for Example 2.

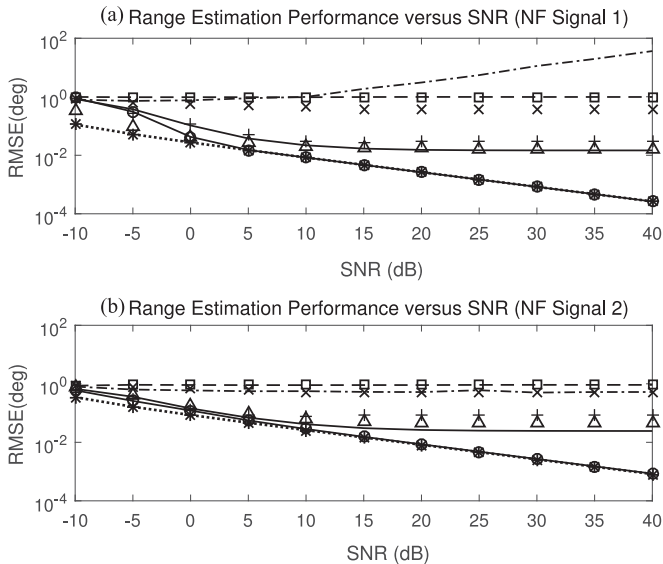


Fig. 5. The RMSEs of the estimated ranges of two NF signals versus the SNR (dashed line: MPL; “x”: SDM; dash-dotted line: GESPR; “ Δ ”: OPMUSIC; “ \square ”: OPMUGE; “+”: G-MUSIC; solid line: LOFNS w/o iteration; solid line with “o”: LOFNS; “*”: theoretical RMSE of LOFNS; and dotted line: CRB) for Example 1.

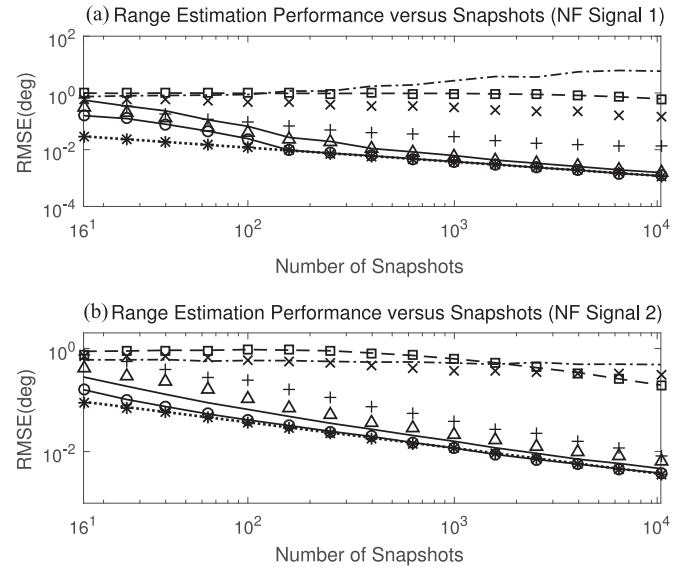


Fig. 7. The RMSEs of the estimated ranges of two NF signals versus the number of snapshots (dashed line: MPL; “x”: SDM; dash-dotted line: GESPR; “ Δ ”: OPMUSIC; “ \square ”: OPMUGE; “+”: G-MUSIC; solid line: LOFNS w/o iteration; solid line with “o”: LOFNS; “*”: theoretical RMSE of LOFNS; and dotted line: CRB) for Example 2.

$\hat{\theta}_1$, $\hat{\theta}_3$ and $\{\hat{r}_k\}_{k=3}^4$ with respect to the number of snapshots are shown in Figs. 6 and 7, respectively.

From Fig. 6(a), we readily find that the proposed LOFNS has the similar estimation performance as the MPL [36], the SDM [38], the OPMUSIC [41], the G-MUSIC [55], and the OPMUGE [43] and is superior to the GESPR [39] for the DOA estimation of FF signals, though the eigendecomposition is used in these existing methods. However, as discussed in Section III-E, when the number of snapshots N is not sufficiently large enough even though the SNR is high, the nonzero residual correlations in

$\hat{\mathbf{R}}_s$ and $\hat{\mathbf{R}}_{sfn}$ will degrade the DOA and range estimation of NF signals. As shown in Figs. 6(b) and 7, we can see that the averaged RMSEs of the estimated DOAs and ranges of NF signals obtained by the proposed LOFNS without iteration is rather large, when the number of snapshots is small. By using the presented alternating iterative scheme with the accessible data, the estimation accuracy of the oblique projection operator and the NF location parameters are improved, and hence the aforementioned “saturation behavior” is overcome, where the difference between the LOFNS with iteration and the LOFNS without

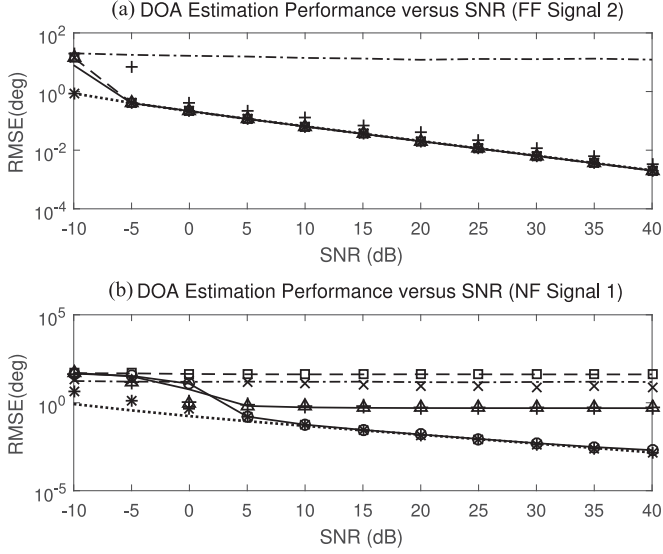


Fig. 8. The RMSEs of the estimated DOAs of (a) FF and (b) NF signals versus the SNR (dashed line: MPL; “×”: SDM; dash-dotted line: GESPR; “△”: OPMUSIC; “□”: OPMUGE; “+”: G-MUSIC; solid line: LOFNS w/o iteration; solid line with “o”: LOFNS; “*”: theoretical RMSE of LOFNS; and dotted line: CRB) for Example 3.

iteration becomes less as the number of snapshots becomes sufficiently large. Moreover, the LOFNS with iteration generally outperforms the aforementioned methods [36], [38], [39], [41], [43], [55]. Additionally, the derived theoretical RMSEs nearly coincide with the empirical RMSEs for larger number of snapshots and generally are very close to the CRBs, while they decrease monotonically with the increasing number of snapshots as analyzed in Section IV.

Example 3—Performance versus Signal Separation: The simulation conditions are similar to those in Example 1, except that two FF signals are located at $(-43^\circ, \infty)$ and $(17^\circ, \infty)$, while two NF signals are located at $(17^\circ, 3.0\lambda)$ and $(54^\circ, 4.4\lambda)$, respectively, i.e., one FF signal $s_2(n)$ and one NF signal $s_3(n)$ have the same DOA $\theta_2 = \theta_3 = 17^\circ$.

The averaged RMSEs of the estimated DOA $\hat{\theta}_2$ of one FF signal and the estimated DOA $\hat{\theta}_3$ of one NF signal in terms of the SNR and the number of snapshots are displayed in Figs. 8 and 9, individually. Obviously for the DOA estimation of the FF signal $s_2(n)$, the proposed LOFNS performs well as the existing localization methods with eigendecomposition such as the MPL [36], the SDM [38], the OPMUSIC [41], and the OPMUGE [43] and outperforms the GESPR [39] and the G-MUSIC [55]. Even though the NF signal $s_3(n)$ impinges the array with the same DOA as the FF signal $s_2(n)$, the LOFNS with alternating iterative scheme can estimate the DOA θ_3 with smaller RMSEs at relatively low SNRs or with relatively small number of snapshots compared to the methods [36], [38], [41], [39], [43], and [55] as observed in previous examples.

VI. CONCLUSION

A new subspace-based method called LOFNS was proposed for localization of the mixed FF and NF signals impinging on a symmetrical ULA, and it has two advantages: (1) the computationally burdensome eigendecomposition is avoided efficiently, and (2) the impact of finite array data is alleviated effectively.

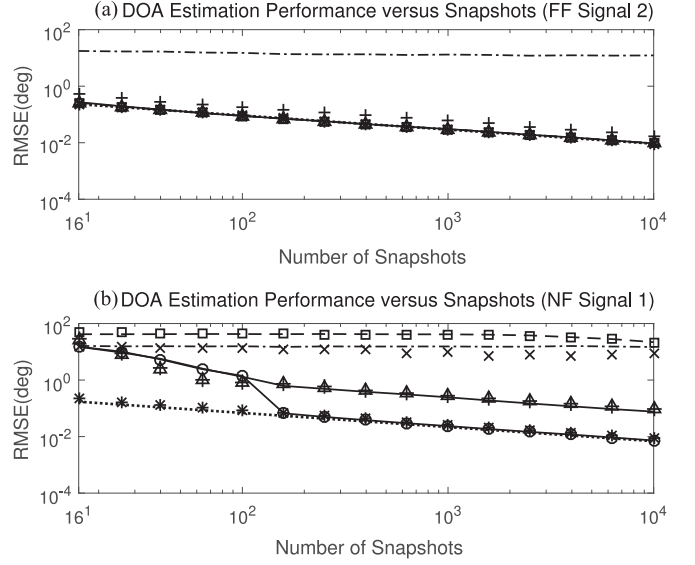


Fig. 9. The RMSEs of the estimated DOAs of (a) FF and (b) NF signals versus the number of snapshots (dashed line: MPL; “×”: SDM; dash-dotted line: GESPR; “△”: OPMUSIC; “□”: OPMUGE; “+”: G-MUSIC; solid line: LOFNS w/o iteration; solid line with “o”: LOFNS; “*”: theoretical RMSE of LOFNS; and dotted line: CRB) for Example 3.

The statistical performance of the LOFNS was studied, and the effectiveness of the LOFNS and the theoretical analysis were verified through numerical examples.

APPENDIX A PROOF OF THEOREM 1

As studied in [64], [65], [49], [11], the first-order expression for the estimation error $\Delta\theta_k \triangleq \hat{\theta}_k - \theta_k$ of FF signals can be obtained as

$$\Delta\theta_k \approx -\frac{f'(\theta_k)}{f''(\theta_k)} \approx -\frac{\text{Re}\left\{\mathbf{d}_f^H(\theta)\mathbf{\Pi}_{\hat{Q}}\mathbf{a}_f(\theta)\right\}}{\mathbf{d}_f^H(\theta)\mathbf{\Pi}_Q\mathbf{d}_f(\theta)} \quad (\text{A1})$$

where a first-order approximation of the estimated orthogonal projector $\mathbf{\Pi}_{\hat{Q}}$ in (A1) is given by [11], [64]

$$\mathbf{\Pi}_{\hat{Q}} \approx (\hat{Q} - Q)(Q^H Q)^{-1}Q^H + Q(Q^H Q)^{-1} \cdot (\hat{Q} - Q)^H + (Q^H \hat{Q})^{-1}Q^H. \quad (\text{A2})$$

By using the fact that $Q^H \mathbf{a}_f(\theta_k) = \mathbf{0}_{(2M+1-K) \times 1}$ and substituting (A2) into (A1), the estimation error $\Delta\theta_k$ can be approximated as

$$\begin{aligned} \Delta\theta_k &\approx -\frac{\text{Re}\left\{\mathbf{d}_f^H(\theta_k)Q(Q^H Q)^{-1}\hat{Q}^H \mathbf{a}_f(\theta_k)\right\}}{\mathbf{d}_f^H(\theta)\mathbf{\Pi}_Q\mathbf{d}_f(\theta)} \\ &= -\frac{\text{Re}\{\mu_k\}}{H_{fkk}} \end{aligned} \quad (\text{A3})$$

where

$$\begin{aligned} \mu_k &\triangleq \mathbf{d}_f^H(\theta_k)Q(Q^H Q)^{-1}\hat{Q}^H \mathbf{a}_f(\theta_k) \\ &= \mathbf{d}_f^H(\theta_k)Q(Q^H Q)^{-1}\tilde{P}^H \mathbf{a}_{f1}(\theta_k) \end{aligned} \quad (\text{A4})$$

where $\mathbf{a}_{f1}(\theta_k)$ denotes the k column of \mathbf{A}_1 with $k = 1, 2, \dots, K_1$, and

$$\begin{aligned} \tilde{\mathbf{P}}^H &\triangleq \hat{\mathbf{P}}^H - \mathbf{P}^H \\ &= (\hat{\mathbf{R}}_2 \hat{\mathbf{R}}_1^H - \mathbf{P}^H \hat{\mathbf{R}}_1 \hat{\mathbf{R}}_1^H) (\hat{\mathbf{R}}_1 \hat{\mathbf{R}}_1^H)^{-1} \\ &\approx -\mathbf{Q}^H \hat{\mathbf{R}} \hat{\mathbf{R}}_1^H (\hat{\mathbf{R}}_1 \hat{\mathbf{R}}_1^H)^{-1} \end{aligned} \quad (\text{A5})$$

where $\mathbf{Q}^H \bar{\mathbf{R}} = \mathbf{Q}^H \mathbf{A} \mathbf{R}_s \mathbf{A}^H = \mathbf{O}_{(2M+1-K) \times (2M+1)}$ is used. By substituting (A5) into (A4) and noting that $\hat{\mathbf{R}} = \hat{\mathbf{R}} - \hat{\sigma}^2 \mathbf{I}_{2M+1}$, we have

$$\begin{aligned} \mu_k &= -\mathbf{d}_f^H(\theta_k) \mathbf{\Pi}_Q \hat{\mathbf{R}} \hat{\mathbf{R}}_1^H (\hat{\mathbf{R}}_1 \hat{\mathbf{R}}_1^H)^{-1} \mathbf{a}_{f1}(\theta_k) \\ &= -\mathbf{g}_f^H(\theta_k) \hat{\mathbf{R}} \mathbf{h}_f(\theta_k) + \hat{\sigma}^2 \mathbf{g}_f^H(\theta_k) \mathbf{h}_f(\theta_k) \\ &= -\frac{1}{N} \sum_{n=1}^N \mathbf{x}^H(n) \mathbf{M}_k \mathbf{x}(n) \end{aligned} \quad (\text{A6})$$

where the fact that $\mathbf{Q}^H \bar{\mathbf{R}}_1^H = \mathbf{O}_{(2M+1-K) \times K}$ and $\mathbf{g}_f^H(\theta_k) \cdot \mathbf{h}_f(\theta_k) = 0$ are used.

Since the estimate $\hat{\theta}_k$ is consistent, from (A3), the MSE (or variance) of the estimation error $\Delta\theta_k$ is given by

$$\begin{aligned} \text{MSE}(\hat{\theta}_k) &\triangleq E\{(\Delta\theta_k)^2\} = \text{var}(\hat{\theta}_k) \\ &\approx \frac{1}{2H_{fkk}^2} \text{Re}\{E\{\mu_k^2\} + E\{|\mu_k|^2\}\} \end{aligned} \quad (\text{A7})$$

where we use the fact that $\text{Re}\{\mu_i\} \text{Re}\{\mu_k\} = 0.5(\text{Re}\{\mu_i \mu_k\} + \text{Re}\{\mu_i \mu_k^*\})$ for implicitity. Under the basic assumptions on the data model and the well-known formula for the expectation of four Gaussian random variables with zero-mean (e.g., [66])

$$\begin{aligned} E\{\mathbf{A} \mathbf{b} \mathbf{c}^T \mathbf{D}\} &= E\{\mathbf{A} \mathbf{b}\} E\{\mathbf{c}^T \mathbf{D}\} + E\{\mathbf{c}^T \otimes \mathbf{A}\} \\ &\quad \cdot E\{\mathbf{D} \otimes \mathbf{b}\} + E\{\mathbf{A} \mathbf{E}\{\mathbf{b} \mathbf{c}^T\} \mathbf{D}\} \end{aligned} \quad (\text{A8})$$

by considering the fact that \mathbf{Q} spans the null space of \mathbf{A} (i.e., $\mathbf{Q}^H \mathbf{A} = \mathbf{O}_{(2M+1-K) \times K}$), from (A6), we can get

$$\begin{aligned} E\{\mu_k^2\} &= \frac{1}{N^2} E\left\{ \sum_{t=1}^N \sum_{n=1}^N \mathbf{x}^H(t) \mathbf{M}_k \mathbf{x}(t) \mathbf{x}^H(n) \mathbf{M}_k \mathbf{x}(n) \right\} \\ &= \frac{1}{N^2} \sum_{t=1}^N \sum_{n=1}^N \left(E\{\mathbf{x}^H(t) \mathbf{M}_k \mathbf{x}(t)\} E\{\mathbf{x}^H(n) \mathbf{M}_k \mathbf{x}(n)\} \right. \\ &\quad + E\{\mathbf{x}^H(t) \otimes \mathbf{x}^H(t) \mathbf{M}_k\} E\{\mathbf{M}_k \mathbf{x}(n) \otimes \mathbf{x}(n)\} \\ &\quad \left. + E\{\mathbf{x}^H(t) \mathbf{M}_k E\{\mathbf{x}(t) \mathbf{x}^H(n)\} \mathbf{M}_k \mathbf{x}(n)\} \right) \\ &= \text{tr}\{\mathbf{M}_k \mathbf{R}\}^2 + 0 + \frac{1}{N} \text{tr}\{(\mathbf{M}_k \mathbf{R})^2\} = 0 \end{aligned} \quad (\text{A9})$$

$$\begin{aligned} E\{|\mu_k|^2\} &= \frac{1}{N^2} E\left\{ \sum_{t=1}^N \sum_{n=1}^N \mathbf{x}^H(t) \mathbf{M}_k \mathbf{x}(t) \mathbf{x}^T(n) \mathbf{M}_k^* \mathbf{x}^*(n) \right\} \\ &= \frac{1}{N^2} \sum_{t=1}^N \sum_{n=1}^N \left(E\{\mathbf{x}^H(t) \mathbf{M}_k \mathbf{x}(t)\} E\{\mathbf{x}^T(n) \mathbf{M}_k^* \mathbf{x}^*(n)\} \right. \\ &\quad + E\{\mathbf{x}^T(n) \otimes \mathbf{x}^H(t) \mathbf{M}_k\} E\{\mathbf{M}_k^* \mathbf{x}^*(n) \otimes \mathbf{x}(t)\} \\ &\quad \left. + E\{\mathbf{x}^H(t) \mathbf{M}_k E\{\mathbf{x}(t) \mathbf{x}^T(n)\} \mathbf{M}_k^* \mathbf{x}^*(n)\} \right) \\ &= \frac{1}{N} \text{vec}(\mathbf{R})^H (\mathbf{M}_k^* \otimes \mathbf{M}_k) \text{vec}(\mathbf{R}) \end{aligned} \quad (\text{A10})$$

where the facts $\mathbf{M}_k \mathbf{R} = \mathbf{O}_{(2M+1) \times (2M+1)}$, $(\mathbf{A} \otimes \mathbf{B})(\mathbf{C} \otimes \mathbf{D}) = (\mathbf{A} \mathbf{C}) \otimes (\mathbf{B} \mathbf{D})$, and $(\mathbf{A} \otimes \mathbf{B})^T = \mathbf{A}^T \otimes \mathbf{B}^T$ are used.

Therefore, by substituting (A9) and (A10) into (A7) and performing some straightforward manipulations, the asymptotic MSE expression $\text{MSE}(\hat{\theta}_k)$ in (47) of the estimated DOAs of FF signals can be readily obtained. ■

APPENDIX B PROOF OF THEOREM 2

Similar to the derivations for the FF signals in Appendix A, the estimation error $\{\Delta\theta_k\}_{k=K_1+1}^K$ for the NF signals is approximately given by

$$\begin{aligned} \Delta\theta_k &\approx -\frac{\text{Re}\{\mathbf{d}_n^H(\theta_k) \bar{\mathbf{Q}} (\bar{\mathbf{Q}}^H \bar{\mathbf{Q}})^{-1} \hat{\mathbf{Q}}^H \mathbf{a}_n(\theta_k)\}}{\mathbf{d}_n^H(\theta) \mathbf{\Pi}_{\bar{\mathbf{Q}}} \mathbf{d}_n(\theta)} \\ &= -\frac{\text{Re}\{\lambda_k\}}{H_{nkk}} \end{aligned} \quad (\text{B1})$$

where

$$\begin{aligned} \lambda_k &\triangleq \mathbf{d}_n^H(\theta_k) \bar{\mathbf{Q}} (\bar{\mathbf{Q}}^H \bar{\mathbf{Q}})^{-1} \hat{\mathbf{Q}}^H \mathbf{a}_n(\theta_k) \\ &= -\mathbf{d}_n^H(\theta_k) \mathbf{\Pi}_{\bar{\mathbf{Q}}} (\mathbf{T}_{n1} \mathbf{T}_{n1}^H)^{-1} \mathbf{a}_{n1}(\theta_k) \\ &= -\mathbf{g}_n^H(\theta_k) \hat{\mathbf{T}}_n \mathbf{h}_n(\theta_k). \end{aligned} \quad (\text{B2})$$

From (13), and (49)–(52), the estimated matrix $\hat{\mathbf{R}}_n$ of \mathbf{R}_n in (26) corresponding to the NF signals is given by

$$\begin{aligned} \hat{\mathbf{R}}_n &= \sum_{k=K_1+1}^K \mathbf{B}_k \hat{\mathbf{R}} \mathbf{B}_k^H \\ &= \sum_{k=K_1+1}^K \left(\mathbf{B}_k \hat{\mathbf{R}} \mathbf{B}_k^H - \hat{\sigma}^2 \mathbf{B}_k \mathbf{B}_k^H \right) \end{aligned} \quad (\text{B3})$$

and the estimated anti-diagonal elements $\hat{r}_n(p)$ of $\hat{\mathbf{R}}_n$ can be obtained by

$$\begin{aligned} \hat{r}_n(p) &= \sum_{k=K_1+1}^K \left(\frac{1}{N} \sum_{n=1}^N \mathbf{b}_{p-M-1}^{(k)T} \mathbf{x}(n) \mathbf{x}^H(n) \mathbf{b}_{M+1-p}^{(k)*} \right. \\ &\quad \left. - \hat{\sigma}^2 \mathbf{b}_{p-M-1}^{(k)T} \mathbf{b}_{M+1-p}^{(k)*} \right). \end{aligned} \quad (\text{B4})$$

Then we can obtain the estimated matrix $\hat{\mathbf{T}}_n$ of the Toeplitz correlation matrix \mathbf{T}_n in (29) as shown in (B5) shown at the bottom of this page, and after some straightforward manipulations, we can reexpress $\hat{\mathbf{T}}_n$ in (B5) compactly as

$$\hat{\mathbf{T}}_n = \frac{1}{N} \sum_{n=1}^N (\mathbf{I}_{M+1} \otimes \mathbf{x}^H(n)) \mathbf{C}(\mathbf{I}_{M+1} \otimes \mathbf{x}(n)) - \hat{\sigma}^2 \tilde{\mathbf{B}}. \quad (\text{B6})$$

Further from (12), the estimated noise variance $\hat{\sigma}^2$ can be formulated as

$$\hat{\sigma}^2 = \frac{1}{2M+1-2K} \text{Re} \left\{ \sum_{n=1}^N \mathbf{x}^H(n) \mathbf{M} \mathbf{x}(n) \right\}. \quad (\text{B7})$$

Hence by inserting (B6) and (B7) into (B2), we have

$$\lambda_k = \lambda_{k1} - \lambda_{k2} \quad (\text{B8})$$

where

$$\begin{aligned} \lambda_{k1} &= -\frac{1}{N} \sum_{t=1}^N \mathbf{g}_n^H(\theta_k) (\mathbf{I}_{M+1} \otimes \mathbf{x}^H(t)) \\ &\quad \cdot \mathbf{C}(\mathbf{I}_{M+1} \otimes \mathbf{x}(t)) \mathbf{h}_n(\theta_k) \\ &= -\frac{1}{N} \sum_{t=1}^N \mathbf{x}^H(t) (\mathbf{g}_n^H(\theta_k) \otimes \mathbf{I}_{2M+1}) \\ &\quad \cdot \mathbf{C}(\mathbf{h}_n(\theta_k) \otimes \mathbf{I}_{2M+1}) \mathbf{x}(t) \\ &= -\frac{1}{N} \sum_{t=1}^N \mathbf{x}^H(t) \bar{\mathbf{M}}_k \mathbf{x}(t) \\ \lambda_{k2} &= -\frac{1}{2M+1-2K} \\ &\quad \cdot \mathbf{g}_n^H(\theta_k) \tilde{\mathbf{B}} \mathbf{h}_n(\theta_k) \text{Re} \left\{ \frac{1}{N} \sum_{n=1}^N \mathbf{x}^H(n) \mathbf{M} \mathbf{x}(n) \right\}. \end{aligned} \quad (\text{B9}) \quad (\text{B10})$$

Additionally by using the fact that

$$\begin{aligned} \text{Re}\{\lambda_k\} &= \text{Re}\{\lambda_{k1}\} - \xi_k \text{Re}\{\bar{\lambda}_{k2}\} \\ &= \text{Re}\{\lambda_{k1} - \xi_k \bar{\lambda}_{k2}\} \end{aligned} \quad (\text{B11})$$

and by defining $\bar{\lambda}_k \triangleq \lambda_{k1} - \xi_k \bar{\lambda}_{k2}$, we have

$$\text{Re}\{\bar{\lambda}_k\} = \text{Re}\{\lambda_k\}. \quad (\text{B12})$$

where $\bar{\lambda}_{k2}$ is given by

$$\bar{\lambda}_{k2} = -\frac{1}{N} \sum_{t=1}^N \mathbf{x}^H(t) \mathbf{M} \mathbf{x}(t). \quad (\text{B13})$$

Thus from (B1) and (B12), the MSE (or variance) of the estimation error $\Delta\theta_k$ is given by

$$\begin{aligned} \text{MSE}(\hat{\theta}_k) &\triangleq E\{(\Delta\theta_k)^2\} = \text{var}(\hat{\theta}_k) \\ &\approx \frac{1}{2H_{nkk}^2} \text{Re}\{E\{\bar{\lambda}_k^2\} + E\{|\bar{\lambda}_k|^2\}\}. \end{aligned} \quad (\text{B14})$$

From (B12), the two terms of $\text{MSE}(\hat{\theta}_k)$ in (B14) can be obtained as

$$E\{\bar{\lambda}_k^2\} = E\{\lambda_{k1}^2 + \xi_k^2 \bar{\lambda}_{k2}^2 - 2\xi_k \lambda_{k1} \bar{\lambda}_{k2}\} \quad (\text{B15})$$

$$\begin{aligned} E\{|\bar{\lambda}_k|^2\} &= E\{|\lambda_{k1}|^2 - \xi_k \lambda_{k1} \bar{\lambda}_{k2}^* - \xi_k \bar{\lambda}_{k2} \lambda_{k1}^* \\ &\quad + \xi_k^2 |\bar{\lambda}_{k2}|^2\} \end{aligned} \quad (\text{B16})$$

where

$$\begin{aligned} E\{\lambda_{k1}^2\} &= \frac{1}{N^2} E \left\{ \sum_{t=1}^N \sum_{n=1}^N \mathbf{x}^H(t) \bar{\mathbf{M}}_k \mathbf{x}(t) \mathbf{x}^H(n) \bar{\mathbf{M}}_k \mathbf{x}(n) \right\} \\ &= \frac{1}{N^2} \sum_{t=1}^N \sum_{n=1}^N \left(E\{\mathbf{x}^H(t) \bar{\mathbf{M}}_k \mathbf{x}(t)\} E\{\mathbf{x}^H(n) \bar{\mathbf{M}}_k \mathbf{x}(n)\} \right. \\ &\quad + E\{\mathbf{x}^H(t) \otimes \mathbf{x}^H(t) \bar{\mathbf{M}}_k\} E\{\bar{\mathbf{M}}_k \mathbf{x}(n) \otimes \mathbf{x}(n)\} \\ &\quad \left. + E\{\mathbf{x}^H(t) \bar{\mathbf{M}}_k E\{\mathbf{x}(t) \mathbf{x}^H(n)\} \bar{\mathbf{M}}_k \mathbf{x}(n)\} \right) \\ &= \text{tr}\{\bar{\mathbf{M}}_k \mathbf{R}\}^2 + 0 + \frac{1}{N} \text{tr}\{(\bar{\mathbf{M}}_k \mathbf{R})^2\} \end{aligned} \quad (\text{B17})$$

$$\begin{aligned} E\{\bar{\lambda}_{k2}^2\} &= \frac{1}{N^2} E \left\{ \sum_{t=1}^N \sum_{n=1}^N \mathbf{x}^H(t) \mathbf{M} \mathbf{x}(t) \mathbf{x}^H(n) \mathbf{M} \mathbf{x}(n) \right\} \\ &= \frac{1}{N^2} \sum_{t=1}^N \sum_{n=1}^N \left(E\{\mathbf{x}^H(t) \mathbf{M} \mathbf{x}(t)\} E\{\mathbf{x}^H(n) \mathbf{M} \mathbf{x}(n)\} \right. \\ &\quad + E\{\mathbf{x}^H(t) \otimes \mathbf{x}^H(t) \mathbf{M}\} E\{\mathbf{M} \mathbf{x}(n) \otimes \mathbf{x}(n)\} \\ &\quad \left. + E\{\mathbf{x}^H(t) \mathbf{M} E\{\mathbf{x}(t) \mathbf{x}^H(n)\} \mathbf{M} \mathbf{x}(n)\} \right) \\ &= \text{tr}\{\mathbf{M} \mathbf{R}\}^2 + 0 + \frac{1}{N} \text{tr}\{(\mathbf{M} \mathbf{R})^2\} \end{aligned} \quad (\text{B18})$$

$$\begin{aligned} E\{\lambda_{k1} \bar{\lambda}_{k2}\} &= \frac{1}{N^2} E \left\{ \sum_{t=1}^N \sum_{n=1}^N \mathbf{x}^H(t) \bar{\mathbf{M}}_k \mathbf{x}(t) \mathbf{x}^H(n) \mathbf{M} \mathbf{x}(n) \right\} \end{aligned}$$

$$\hat{\mathbf{T}}_n = \frac{1}{N} \sum_{t=1}^N \sum_{k=K_1+1}^K \begin{bmatrix} \mathbf{b}_0^{(k)T} \mathbf{x}(n) \mathbf{x}^H(n) \mathbf{b}_0^{(k)*}, & \mathbf{b}_{-1}^{(k)T} \mathbf{x}(n) \mathbf{x}^H(n) \mathbf{b}_1^{(k)*}, & \dots & \mathbf{b}_{-M}^{(k)T} \mathbf{x}(n) \mathbf{x}^H(n) \mathbf{b}_M^{(k)*} \\ \mathbf{b}_1^{(k)T} \mathbf{x}(n) \mathbf{x}^H(n) \mathbf{b}_{-1}^{(k)*}, & \mathbf{b}_0^{(k)T} \mathbf{x}(n) \mathbf{x}^H(n) \mathbf{b}_0^{(k)*}, & \dots & \mathbf{b}_{-M+1}^{(k)T} \mathbf{x}(n) \mathbf{x}^H(n) \mathbf{b}_{M-1}^{(k)*} \\ \vdots & \vdots & \ddots & \vdots \\ \mathbf{b}_M^{(k)T} \mathbf{x}(n) \mathbf{x}^H(n) \mathbf{b}_{-M}^{(k)*}, & \mathbf{b}_{M-1}^{(k)T} \mathbf{x}(n) \mathbf{x}^H(n) \mathbf{b}_{-M+1}^{(k)*}, & \dots & \mathbf{b}_0^{(k)T} \mathbf{x}(n) \mathbf{x}^H(n) \mathbf{b}_0^{(k)*} \end{bmatrix} - \hat{\sigma}^2 \tilde{\mathbf{B}} \quad (\text{B5})$$

$$\begin{aligned}
&= \frac{1}{N^2} \sum_{t=1}^N \sum_{n=1}^N \left(E\{\mathbf{x}^H(t) \bar{\mathbf{M}}_k \mathbf{x}(t)\} E\{\mathbf{x}^H(n) \mathbf{M} \mathbf{x}(n)\} \right. \\
&\quad + E\{\mathbf{x}^H(t) \otimes \mathbf{x}^H(t) \bar{\mathbf{M}}_k\} E\{\mathbf{M} \mathbf{x}(n) \otimes \mathbf{x}(t)\} \\
&\quad \left. + E\{\mathbf{x}^H(t) \bar{\mathbf{M}}_k E\{\mathbf{x}(t) \mathbf{x}^H(n)\} \mathbf{M} \mathbf{x}(n)\} \right) \\
&= \text{tr}\{\bar{\mathbf{M}}_k \mathbf{R}\} \text{tr}\{\mathbf{M} \mathbf{R}\} + 0 \\
&\quad + \frac{1}{N} \text{vec}(\mathbf{R})^H (\bar{\mathbf{M}}_k^T \otimes \mathbf{M}) \text{vec}(\mathbf{R}) \quad (\text{B19})
\end{aligned}$$

where the facts that $\text{tr}(\mathbf{A}^T \mathbf{B}) = \text{vec}^T(\mathbf{A}) \text{vec}(\mathbf{B})$ and $\text{vec}(\mathbf{A} \mathbf{X} \mathbf{B}) = (\mathbf{B}^T \otimes \mathbf{A}) \text{vec}(\mathbf{X})$ are used, while

$$\begin{aligned}
&E\{|\lambda_{k1}|^2\} \\
&= \frac{1}{N^2} E \left\{ \sum_{t=1}^N \sum_{n=1}^N \mathbf{x}^H(t) \bar{\mathbf{M}}_k \mathbf{x}(t) \mathbf{x}^T(n) \bar{\mathbf{M}}_k^* \mathbf{x}^*(n) \right\} \\
&= \frac{1}{N^2} \sum_{t=1}^N \sum_{n=1}^N \left(E\{\mathbf{x}^H(t) \bar{\mathbf{M}}_k \mathbf{x}(t)\} E\{\mathbf{x}^T(n) \bar{\mathbf{M}}_k^* \mathbf{x}^*(n)\} \right. \\
&\quad + E\{\mathbf{x}^T(n) \otimes \mathbf{x}^H(t) \bar{\mathbf{M}}_k\} E\{\bar{\mathbf{M}}_k^* \mathbf{x}^*(n) \otimes \mathbf{x}(t)\} \\
&\quad \left. + E\{\mathbf{x}^H(t) \bar{\mathbf{M}}_k E\{\mathbf{x}(t) \mathbf{x}^T(n)\} \bar{\mathbf{M}}_k^* \mathbf{x}^*(n)\} \right) \\
&= \text{tr}\{\bar{\mathbf{M}}_k \mathbf{R}\} \text{tr}\{\bar{\mathbf{M}}_k \mathbf{R}\}^* \\
&\quad + \frac{1}{N} \text{vec}(\mathbf{R})^H (\bar{\mathbf{M}}_k^* \otimes \bar{\mathbf{M}}_k) \text{vec}(\mathbf{R}) \quad (\text{B20})
\end{aligned}$$

$$\begin{aligned}
&E\{|\bar{\lambda}_{k2}|^2\} \\
&= \frac{1}{N^2} E \left\{ \sum_{t=1}^N \sum_{n=1}^N \mathbf{x}^H(t) \mathbf{M} \mathbf{x}(t) \mathbf{x}^T(n) \mathbf{M}^* \mathbf{x}^*(n) \right\} \\
&= \frac{1}{N^2} \sum_{t=1}^N \sum_{n=1}^N \left(E\{\mathbf{x}^H(t) \mathbf{M} \mathbf{x}(t)\} E\{\mathbf{x}^T(n) \mathbf{M}^* \mathbf{x}^*(n)\} \right. \\
&\quad + E\{\mathbf{x}^T(n) \otimes \mathbf{x}^H(t) \mathbf{M}\} E\{\mathbf{M}^* \mathbf{x}^*(n) \otimes \mathbf{x}(t)\} \\
&\quad \left. + E\{\mathbf{x}^H(t) \mathbf{M} E\{\mathbf{x}(t) \mathbf{x}^T(n)\} \mathbf{M}^* \mathbf{x}^*(n)\} \right) \\
&= \text{tr}\{\mathbf{M} \mathbf{R}\} \text{tr}\{\mathbf{M} \mathbf{R}\}^* \\
&\quad + \frac{1}{N} \text{vec}(\mathbf{R})^H (\mathbf{M}^* \otimes \mathbf{M}) \text{vec}(\mathbf{R}) \quad (\text{B21})
\end{aligned}$$

$$\begin{aligned}
&E\{\lambda_{k1} \bar{\lambda}_{k2}^*\} \\
&= \frac{1}{N^2} E \left\{ \sum_{t=1}^N \sum_{n=1}^N \mathbf{x}^H(t) \bar{\mathbf{M}}_k \mathbf{x}(t) \mathbf{x}^T(n) \mathbf{M}^* \mathbf{x}^*(n) \right\} \\
&= \frac{1}{N^2} \sum_{t=1}^N \sum_{n=1}^N \left(E\{\mathbf{x}^H(t) \bar{\mathbf{M}}_k \mathbf{x}(t)\} E\{\mathbf{x}^T(n) \mathbf{M}^* \mathbf{x}^*(n)\} \right. \\
&\quad + E\{\mathbf{x}^T(n) \otimes \mathbf{x}^H(t) \bar{\mathbf{M}}_k\} E\{\mathbf{M}^* \mathbf{x}^*(n) \otimes \mathbf{x}(t)\} \\
&\quad \left. + E\{\mathbf{x}^H(t) \bar{\mathbf{M}}_k E\{\mathbf{x}(t) \mathbf{x}^T(n)\} \mathbf{M}^* \mathbf{x}^*(n)\} \right)
\end{aligned}$$

$$\begin{aligned}
&= \text{tr}\{\bar{\mathbf{M}}_k \mathbf{R}\} \text{tr}\{\mathbf{M} \mathbf{R}\}^* \\
&\quad + \frac{1}{N} \text{vec}(\mathbf{R})^H (\mathbf{M}^* \otimes \bar{\mathbf{M}}_k) \text{vec}(\mathbf{R}). \quad (\text{B22})
\end{aligned}$$

Moreover, we have

$$\begin{aligned}
\text{tr}\{\bar{\mathbf{M}}_k \mathbf{R}\} &= E\{\mathbf{x}^H(n) \bar{\mathbf{M}}_k \mathbf{x}(n)\} \\
&= \mathbf{g}_n^H(\theta_k) \mathbf{T}_n \mathbf{h}_n(\theta_k) + \sigma^2 \mathbf{g}_n^H(\theta_k) \tilde{\mathbf{B}} \mathbf{h}_n(\theta_k) \\
&= \sigma^2 \mathbf{g}_n^H(\theta_k) \tilde{\mathbf{B}} \mathbf{h}_n(\theta_k). \quad (\text{B23})
\end{aligned}$$

Therefore, by inserting (B17)–(B23), (B15) and (B16) into (B14), and performing some straightforward manipulations, MSE($\hat{\theta}_k$) in (48) of the estimated DOAs of NF signals can be readily obtained. ■

ACKNOWLEDGMENT

The authors would like to thank the anonymous reviewers and the associate editor Prof. M. Davenport for their insightful comments and valuable suggestions.

REFERENCES

- [1] H. Krim and M. Viberg, "Two decades of array signal processing research: The parametric approach," *IEEE Signal Process. Mag.*, vol. 13, no. 4, pp. 67–94, Jul. 1996.
- [2] H. L. Van Trees, *Optimum Array Processing, Part IV of Detection, Estimation, and Modulation Theory*. New York, NY, USA: Wiley, 2002.
- [3] D. H. Johnson and D. E. Dudgeon, *Array Signal Processing: Concepts and Techniques*. Upper Saddle River, NJ, USA: Prentice-Hall, 1993.
- [4] *Smart Antennas and Signal Processing for Communications, Biomedical and Radar Systems*. P.R.P. Hoole, Ed. Southampton, U.K.: WIT Press, 2001.
- [5] R. O. Schmidt, "Multiple emitter location and signal parameter estimation," in *Proc. RADC Spectr. Estimation Workshop*, Rome, NY, USA, Oct. 1979, pp. 243–258.
- [6] R. Kumaresan and D. W. Tufts, "Estimating the angels of arrival of multiple plane waves," *IEEE Trans. Aerosp. Electron. Syst.*, vol. AES-19, no. 1, pp. 134–139, Jan. 1983.
- [7] R. Roy and T. Kailath, "ESPRIT—Estimation of signal parameters via rational invariance techniques," *IEEE Trans. Acoust., Speech, Signal Process.*, vol. 37, no. 7, pp. 984–995, Jul. 1989.
- [8] P. Stoica and K. C. Sharman, "Novel eigenanalysis method for direction estimation," *Proc. Inst. Electr. Eng.—F, Radar Signal Process.*, vol. 137, no. 1, pp. 19–26, 1990.
- [9] M. Viberg and B. Ottersten, "Sensor array processing based on subspace fitting," *IEEE Trans. Signal Process.*, vol. 39, no. 5, pp. 1110–1121 1991.
- [10] S. Marcos, A. Marsal, and M. Benider, "The propagator method for sources bearing estimation," *Signal Process.*, vol. 42, no. 2, pp. 121–138, May 1995.
- [11] J. Xin and A. Sano, "Computationally efficient subspace-based method for direction-of-arrival estimation without eigendecomposition," *IEEE Trans. Signal Process.*, vol. 52, no. 4, pp. 876–893, Apr. 2004.
- [12] A. L. Swindlehurst and T. Kailath, "Passive direction-of-arrival and range estimation for near-field sources," in *Proc. IEEE 4th ASSP Workshop Spectr. Estimation Model.*, Minneapolis, MN, USA, Aug. 1988, pp. 123–128.
- [13] A. J. Weiss and B. Friedlander, "Range and bearing estimation using polynomial rooting," *IEEE J. Ocean. Eng.*, vol. 18, no. 2, pp. 130–137, Apr. 1993.
- [14] D. Starer and A. Nehorai, "Passive localization of near-field sources by path following," *IEEE Trans. Signal Process.*, vol. 42, no. 3, pp. 677–680, Mar. 1994.
- [15] Y. D. Huang and M. Barkat, "Near-field multiple source localization by passive sensor array," *IEEE Trans. Antennas Propag.*, vol. 39, no. 7, pp. 968–975, Jul. 1991.
- [16] J. H. Lee, Y. M. Chen, and C.-C. Yeh, "A covariance approximation method for near-field direction finding using a uniform linear array," *IEEE Trans. Signal Process.*, vol. 43, no. 5, pp. 1293–1298, May 1995.

- [17] J.-H. Lee and C.-H. Tung, "Estimating the bearings of near-field cyclostationary signals," *IEEE Trans. Signal Process.*, vol. 50, no. 1, pp. 110–118, Jan. 2002.
- [18] E. Boyer, A. Ferreol, and P. Larzabal, "Simple robust bearing-range source's localization with curved wavefronts," *IEEE Signal Process. Lett.*, vol. 12, no. 6, pp. 457–460, Jun. 2005.
- [19] E. Grosicki, K. Abed-Meraim, and Y. Hua, "A weighted linear prediction method for near-field source localization," *IEEE Trans. Signal Process.*, vol. 53, no. 10, pp. 3651–3660, Oct. 2005.
- [20] Y. Wu, L. Ma, C. Hou, G. Zhang, and J. Li, "Subspace-based method for joint range and DOA estimation of multiple near-field sources," *Signal Process.*, vol. 86, pp. 2129–2133, 2006.
- [21] W. Zhi and M. Y. Chia, "Near-field source localization via symmetric subarrays," *IEEE Signal Process. Lett.*, vol. 14, no. 6, pp. 409–412, Jun. 2007.
- [22] J. Liang and D. Liu, "Passive localization of near-field sources using cumulant," *IEEE Sensors J.*, vol. 9, no. 8, pp. 953–960, Aug. 2009.
- [23] H. Noh and C. Lee, "A covariance approximation method for near-field coherent sources localization using uniform linear array," *IEEE J. Ocean. Eng.*, vol. 40, no. 1, pp. 187–195, Jan. 2015.
- [24] D. B. Ward and G. W. Elko, "Mixed nearfield/farfield beamforming: A new technique for speech acquisition in a reverberant environment," in *Proc. IEEE ASSP Workshop Appl. Signal Process. Audio Acoust.*, New Paltz, NY, USA, Oct. 1997, pp. 19–22.
- [25] G. Arslan and F. A. Sakarya, "A unified neural-network-based speaker localization technique," *IEEE Trans. Neural Netw.*, vol. 11, no. 4, pp. 997–1002, Jul. 2000.
- [26] P. Tichavsky, K. T. Wong, and M. D. Zoltowski, "Near-field/far-field azimuth elevation angle estimation using a single vector-hydrophone," *IEEE Trans. Signal Process.*, vol. 49, no. 11, pp. 2498–2510, Nov. 2001.
- [27] J. M. Mendel, "Tutorial on higher-order statistics (spectra) in signal processing and system theory: Theoretical results and some applications," *Proc. IEEE*, vol. 79, no. 3, pp. 278–305, Mar. 1991.
- [28] W. A. Gardner, "Exploitation of spectral redundancy in cyclostationary signals," *IEEE Signal Process. Mag.*, vol. 8, no. 2, pp. 14–36, Apr. 1991.
- [29] J. Liang and D. Liu, "Passive localization of mixed near-field and far-field sources using two-stage MUSIC algorithm," *IEEE Trans. Signal Process.*, vol. 58, no. 1, pp. 108–120, Jan. 2010.
- [30] B. Wang, J. Liu, and X. Sun, "Mixed sources localization based on sparse signal reconstruction," *IEEE Signal Process. Lett.*, vol. 19, no. 8, pp. 487–490, Aug. 2012.
- [31] B. Wang, Y. Zhao, and J. Liu, "Mixed-order MUSIC algorithm for localization of far-field and near-field sources," *IEEE Signal Process. Lett.*, vol. 20, no. 4, pp. 311–314, Apr. 2013.
- [32] Y. Tian and X. Sun, "Mixed sources localisation using a sparse representation of cumulant vectors," *IET Signal Process.*, vol. 8, no. 6, pp. 606–611, 2014.
- [33] J. Xie, H. Tao, X. Rao, and J. Su, "Passive localization of mixed far-field and near-field sources without estimating the number of sources," *Sensors*, vol. 15, no. 2, pp. 3834–3853, 2015.
- [34] K. Wang, L. Wang, J.-R. Shang, and X.-X. Qu, "Mixed near-field and far-field source localization based on uniform linear array partition," *IEEE Sens. J.*, vol. 16, no. 22, pp. 8083–8090, Nov. 2016.
- [35] G. Liu, X. Sun, Y. Liu, and Y. Qin, "Low-complexity estimation of signal parameters via rotational invariance techniques algorithm for mixed far-field and near-field cyclostationary sources localisation," *IET Signal Process.*, vol. 7, no. 5, pp. 382–388, 2013.
- [36] G. Liu and X. Sun, "Efficient method of passive localization for mixed far-field and near-field sources," *IEEE Antennas Wireless Propag. Lett.*, vol. 12, pp. 902–905, 2013.
- [37] G. Liu and X. Sun, "Two-stage matrix differencing algorithm for mixed far-field and near-field sources classification and localization," *IEEE Sensors J.*, vol. 14, no. 6, pp. 1957–1965, Jun. 2014.
- [38] G. Liu and X. Sun, "Spatial differencing method for mixed far-field and near-field sources localization," *IEEE Signal Process. Lett.*, vol. 21, no. 11, pp. 1331–1335, Nov. 2014.
- [39] J.-J. Jiang, F.-J. Duan, J. Chen, Y.-C. Li, and X.-N. Hua, "Mixed near-field and far-field sources localization using the uniform linear sensor array," *IEEE Sensors J.*, vol. 13, no. 8, pp. 3136–3143, Aug. 2013.
- [40] J.-J. Jiang, F.-J. Duan, and X.-Q. Wang, "An efficient classification method of mixed sources," *IEEE Sensors J.*, vol. 16, no. 10, pp. 3731–3734, May 2016.
- [41] J. He, M. N. S. Swamy, and M. O. Ahmad, "Efficient application of MUSIC algorithm under the coexistence of far-field and near-field sources," *IEEE Trans. Signal Process.*, vol. 60, no. 4, pp. 2066–2070, Apr. 2012.
- [42] B. Wang, Y. Zhao, and J. Liu, "Sparse recovery method for far-field and near-field sources localization using oblique projection," *J. China Univ. Posts Telecommun.*, vol. 20, no. 3, pp. 90–96, 2013.
- [43] W. Si, X. Li, Y. Jiang, and L. Wan, "A novel method based on oblique projection technology for mixed sources estimation," *Math. Problems Eng.*, vol. 2014, 2014, Art. no. 675271.
- [44] F. Gao and A. B. Gershman, "A generalized ESPRIT approach to direction-of-arrival estimation," *IEEE Signal Process. Lett.*, vol. 12, no. 3, pp. 254–257, Mar. 2005.
- [45] G. Wang, J. Xin, J. Wu, J. Wang, N. Zheng, and A. Sano, "New generalized ESPRIT for direction estimation and its mathematical link to RARE method," in *Proc. IEEE 12th Int. Conf. Signal Process.*, Beijing, China, Oct. 2012, pp. 360–363.
- [46] R. T. Behrens and L. L. Scharf, "Signal processing applications of oblique projection operators," *IEEE Trans. Signal Process.*, vol. 42, no. 6, pp. 1413–1424, Jun. 1994.
- [47] R. Boyer and G. Bouleux, "Oblique projection for direction-of-arrival estimation with prior knowledge," *IEEE Trans. Signal Process.*, vol. 56, no. 4, pp. 1374–1387, Apr. 2008.
- [48] M. L. McCloud and L. L. Scharf, "A new subspace identification algorithm for high-resolution DOA estimation," *IEEE Trans. Antennas Propag.*, vol. 50, no. 10, pp. 1382–1389, Oct. 2002.
- [49] H. Tao, J. Xin, J. Wang, N. Zheng, and A. Sano, "Two-dimensional direction estimation for a mixture of noncoherent and coherent signals," *IEEE Trans. Signal Process.*, vol. 63, no. 2, pp. 318–333, Jan. 2015.
- [50] W. Zuo, J. Xin, J. Wang, N. Zheng, and A. Sano, "A computationally efficient source localization method for a mixture of near-field and far-field signals," in *Proc. IEEE Int. Conf. Acoust., Speech, Signal Process.*, Florence, Italy, May 2014, pp. 2276–2280.
- [51] G. H. Golub and C. F. Van Loan, *Matrix Computations*, 2nd ed. Baltimore, MD, USA: John Hopkins Univ. Press, 1989.
- [52] R. B. Barrar and C. H. Wilcox, "On the Fresnel approximation," *IRE Trans. Antennas Propag.*, vol. 6, no. 1, pp. 43–48, 1958.
- [53] H. Tao, J. Xin, J. Wang, N. Zheng, and A. Sano, "Oblique projection based enumeration of mixed noncoherent and coherent narrowband signals," *IEEE Trans. Signal Process.*, vol. 64, no. 16, pp. 4282–4295, Aug. 2016.
- [54] R. Couillet and M. Debbah, "Signal processing in large systems: A new paradigm," *IEEE Signal Process. Mag.*, vol. 30, no. 1, pp. 24–39, Jan. 2013.
- [55] X. Mestre and M. A. Lagunas, "Modified subspace algorithms for DOA estimation with large arrays," *IEEE Trans. Signal Process.*, vol. 56, no. 2, pp. 598–614, Feb. 2008.
- [56] B. A. Johnson, Y. I. Abramovich, and X. Mestre, "MUSIC, G-MUSIC, and maximum-likelihood performance breakdown," *IEEE Trans. Signal Process.*, vol. 56, no. 8, pp. 3944–3958, Aug. 2008.
- [57] X. Mestre, "Improved estimation of eigenvalues and eigenvectors of covariance matrices using their sample estimates," *IEEE Trans. Inf. Theory*, vol. 54, no. 11, pp. 5113–5129, Nov. 2008.
- [58] R. Couillet, F. Pascal, and J. W. Silverstein, "Robust estimates of covariance matrices in the large dimensional regime," *IEEE Trans. Inf. Theory*, vol. 60, no. 11, pp. 7269–7278, Nov. 2014.
- [59] P. Vallet, X. Mestre, and P. Loubaton, "Performance analysis of an improved MUSIC DoA estimator," *IEEE Trans. Signal Process.*, vol. 63, no. 23, pp. 6407–6422, Dec. 2015.
- [60] J. Sanchez-Araujo, and S. Marcos, "Statistical analysis of the propagator method for DOA estimation without eigendecomposition," in *Proc. IEEE 8th Workshop Statistical Signal Array Process.*, Corfu, Greece, Jun. 1996, pp. 570–573.
- [61] T. Bäckström, "Vandermonde factorization of Toeplitz matrices and applications in filtering and warping," *IEEE Trans. Signal Process.*, vol. 61, no. 24, pp. 6257–6263, Dec. 2013.
- [62] Z. Yang, L. Xie, and P. Stoica, "Vandermonde decomposition of multilevel Toeplitz matrices with application to multidimensional super-resolution," *IEEE Trans. Inf. Theory*, vol. 62, no. 6, pp. 3685–3701, Jun. 2016.
- [63] H. Liu and W. Zhang, "A novel near-field localization method based on second order statistics," in *Proc. 2008 Int. Congr. Image Signal Process.*, Sanya, China, May 2008, vol. 5, pp. 29–33.
- [64] P. Stoica and T. Söderström, "Statistical analysis of a subspace method for bearing estimation without eigendecomposition," *Proc. Inst. Electr. Eng.—F, Radar Signal Process.*, vol. 139, no. 4, pp. 301–305, 1992.
- [65] G. Wang, J. Xin, N. Zheng, and A. Sano, "Computationally efficient subspace-based method for two-dimensional direction estimation with L-shaped array," *IEEE Trans. Signal Process.*, vol. 59, no. 7, pp. 3197–3212, Jul. 2011.

- [66] P. H. M. Janssen and P. Stoica, "On the expectation of the product of four matrix-valued Gaussian random variables," *IEEE Trans. Autom. Control*, vol. 33, no. 9, pp. 867–870, Sep. 1988.
- [67] X. Xu, Z. Ye, Y. Zhang, and C. Chang, "A deflation approach to direction of arrival estimation for symmetric uniform linear array," *IEEE Antennas Wireless Propag. Lett.*, vol. 5, pp. 486–489, 2006.
- [68] X. Xu, Z. Ye, and J. Peng, "Method of direction-of-arrival estimation for uncorrelated, partially correlated and coherent sources," *IET Microw. Antennas Propag.*, vol. 1, no. 4, pp. 949–954, 2007.
- [69] X. Xu, Z. Ye, and Y. Zhang, "DOA estimation for mixed signals in the presence of mutual coupling," *IEEE Trans. Signal Process.*, vol. 57, no. 9, pp. 3523–3532, Sep. 2009.
- [70] L. Wan, G. Han, L. Shu, and N. Feng, "The critical patients localization algorithm using sparse representation for mixed signals in emergency healthcare system," *IEEE Syst. J.*, vol. 12, no. 1, pp. 52–63, Mar. 2018.
- [71] H. Hou, X. Mao, and Y. Liu, "Oblique projection for direction-of-arrival estimation of hybrid completely polarised and partially polarised signals with arbitrary polarimetric array configuration," *IET Signal Process.*, vol. 11, no. 8, pp. 893–900, 2017.



Weiliang Zuo received the B.E. degree in electrical engineering from Xi'an Jiaotong University, Xi'an, China, in 2010. He is currently working toward the Ph.D. degree with the Department of Control Science and Engineering, Xi'an Jiaotong University. During 2016 to 2017, he was a visiting student in the School of Electrical and Computer Engineering with the Georgia Institute of Technology. His current research interests include array and statistical signal processing.



Jingmin Xin (S'92–M'96–SM'06) received the B.E. degree in information and control engineering from Xi'an Jiaotong University, Xi'an, China, in 1988, and the M.S. and Ph.D. degrees in electrical engineering from Keio University, Yokohama, Japan, in 1993 and 1996, respectively. From 1988 to 1990, he was with the Tenth Institute of Ministry of Posts and Telecommunications of China, Xi'an, China. He was with the Communications Research Laboratory, Japan, as an Invited Research Fellow of the Telecommunications Advancement Organization of Japan from 1996 to 1997, and as a Postdoctoral Fellow of the Japan Science and Technology Corporation from 1997 to 1999. He was also a Guest (Senior) Researcher with YRP Mobile Telecommunications Key Technology Research Laboratories Company, Limited, Yokosuka, Japan, from 1999 to 2001. From 2002 to 2007, he was with Fujitsu Laboratories Limited, Yokosuka, Japan. Since 2007, he has been a Professor with Xi'an Jiaotong University. His research interests include adaptive filtering, statistical and array signal processing, system identification, and pattern recognition.



Nanning Zheng (SM'93–F'06) received the Graduated degree from the Department of Electrical Engineering, Xi'an Jiaotong University, Xi'an, China, in 1975, and the M.S. degree in information and control engineering from Xi'an Jiaotong University, in 1981, and the Ph.D. degree in electrical engineering from Keio University, Yokohama, Japan, in 1985. He joined Xi'an Jiaotong University in 1975, and is currently a Professor and the Director of the Institute of Artificial Intelligence and Robotics, Xi'an Jiaotong University. His research interests include computer vision, pattern recognition and image processing, and hardware implementation of intelligent systems. He became a member of the Chinese Academy of Engineering in 1999, and he is the Chinese Representative on the Governing Board of the International Association for Pattern Recognition. He also serves as an Executive Deputy Editor of the *Chinese Science Bulletin*.



Akira Sano (M'89) received the B.E., M.S., and Ph.D. degrees in mathematical engineering and information physics from the University of Tokyo, Tokyo, Japan, in 1966, 1968, and 1971, respectively. In 1971, he joined the Department of Electrical Engineering, Keio University, Yokohama, Japan, where he was a Professor with the Department of System Design Engineering till 2009, and is currently a Professor Emeritus. He is a member of Science Council of Japan since 2005. He was a Visiting Research Fellow with the University of Salford, Salford, U.K., from 1977 to 1978. He is a coauthor of the textbook *State Variable Methods in Automatic Control* (New York, NY, USA: Wiley, 1988). His current research interests include adaptive modeling and design theory in control, signal processing and communication, and applications to control of sounds and vibrations, mechanical systems, and mobile communication systems. He was the recipient of the Kelvin Premium from the Institute of Electrical Engineering in 1986. He is a Fellow of the Society of Instrument and Control Engineers and is a member of the Institute of Electrical Engineering of Japan and the Institute of Electronics, Information and Communications Engineers of Japan. He was the General Co-Chair of the 1999 IEEE Conference of Control Applications and an IPC Chair of the 2004 IFAC Workshop on Adaptation and Learning in Control and Signal Processing. He was the Chair of IFAC Technical Committee on Modeling and Control of Environmental Systems from 1996 to 2001. He has also been the Vice Chair of IFAC Technical Committee on Adaptive Control and Learning since 1999 and has been the Chair of IFAC Technical Committee on Adaptive and Learning Systems since 2002. He was also on the Editorial Board of *Signal Processing*.